Subduction and obduction processes: the fate of oceanic lithosphere revealed by blueschists, eclogites and ophiolites

Philippe Agard, Mathieu Soret, Guillaume Bonnet, Dia Ninkabou, Alexis Plunder, Cécile Prigent, Philippe Yamato

Subduction and obduction processes: the fate of oceanic lithosphere revealed by blueschists, eclogites and ophiolites

P. Agard[1], M. Soret[1,2], G. Bonnet[1], D. Ninkabou[1], A. Plunder[3], C. Prigent[4], P. Yamato[5]

[1]Sorbonne Université, CNRS-INSU, Institut des Sciences de la Terre Paris, ISTeP UMR 7193, F-75005 Paris
[2] Institut des Sciences de la Terre d'Orléans (ISTO), UMR 7327, CNRS–BRGM, Université d'Orléans, 45071, Orléans, France
[3]BRGM, F-45060, Orléans, France
[4]Institut de Physique du Globe de Paris, Sorbonne Paris Cité, Univ. Paris Diderot, CNRS, F-75005 Paris, France
[5]Géosciences Rennes, Université de Rennes 1, CNRS UMR 6118, F-35042 Rennes Cedex, France

Accepted manuscript
In: Compressional Tectonics: Plate Convergence to Mountain Building - Volume 2, Ed. Catlos, Cehmen, Dalziel)

Abstract

Fragments of former oceans are commonly observed in mountain belts: blueschists and eclogites, on the one hand, and ophiolites, on the other hand, are all that remains of ancient oceanic lithosphere. Though volumetrically subordinate, they provide essential insights into past geodynamics and into the processes involved in the formation and destruction of oceanic lithosphere. This contribution apprehends these two types of oceanic fragments jointly and shows the advantage of doing so for understanding the dynamics of oceanic convergence, i.e. subduction and obduction. We examine the intimate relationships between blueschists/eclogites and ophiolites, as well as the similarities and differences in the mechanisms leading to their preservation. While the extensive, unmetamorphosed true ophiolites markedly differ from fragments of oceanic lithosphere offscraped from the slab during subduction, at shallow or great depths, both types record the mechanical behavior and 'hiccups' of the subduction plate boundary. Their preservation also highlights the importance of the evolution of the subduction regime through time, from the onset of intra-oceanic subduction to the cessation of continental subduction.

Keywords: ophiolite, eclogite, subduction, blueschist, obduction, lithosphere

1. Introduction

Blueschists and eclogites have now been collected and studied for more than two centuries (de Saussure, 1804; Ernst, 1971). Ophiolites, at least coined as such, for about fifty years (Coleman, 1971; Dewey, 1976; Moores, 1982). Both represent important milestones for the theory of Plate tectonics. More often than not, however, these rock associations are studied independently. The present contribution provides a short odyssey through these two types of oceanic fragments to precise their intimate links, as well as to show the advantage of studying them jointly for understanding the dynamics of oceanic convergence.

Oceanic lithosphere, formed by partial melting along ocean ridges or by extreme thinning of the mantle, makes up more than 60% of the surface of our planet. Despite this extreme prevalence, ocean floors are younger than ~200 Ma around most of the globe (Fig. 1a; except possibly in the eastern Mediterranean). Oceanic lithosphere is young because it is doomed: most of it, save for a few fragments, irreversibly disappears in convergent zones through the 'subduction' process.

The subduction machine drives ocean recycling and triggers the largest known earthquakes, as well as devastating volcanic eruptions (Stern, 2002; Fig. 1b). Subduction, together with mantle convection (Forsyth and Uyeda, 1975; Coltice et al., 2019), not only governs solid Earth dynamics but fundamentally connects the atmosphere and the biosphere with the deep Earth: water, carbon or any other element of the Mendeleïev table travels down through subduction zones.

Some fragments of oceanic lithosphere nevertheless escape their tragic fate and are preserved as slivers in recent as well as ancient mountain belts. They form oceanic *'sutures'* outlining fossil plate boundaries where former oceans have disappeared (Fig. 1c), and constitute major lithospheric scars. As such, they commonly play an important role in later deformation of the Earth's crust.

The preserved fragments of oceanic lithosphere (mantle, crust, sediments), recognizable through their petrological and structural features, are of two major types: (1) *'ophiolites',* i.e. hundreds of km long fragments with a diagnostic lithological sequence that have largely escaped later metamorphic transformations, thanks to a process called *'obduction'* (Coleman, 1971, Moores, 1982); (2) 'blueschists' or 'eclogites' that have experienced high-pressure low-temperature (HP-LT) metamorphic conditions during subduction to variable depths (Guillot et al., 2004; Federico et al., 2007). Whilst the latter are sometimes referred to as 'ophiolites' (or 'ophiolitic') to underline their oceanic origin, we shall restrict the use of the term ophiolite to the former type for clarity. We will see that this distinction echoes a more fundamental one, related to their mode of emplacement.

The first type of fragment informs us about the detailed constitution of 'pristine' oceanic lithosphere. While surveyed and partly sampled at sea, oceanic lithosphere is conveniently investigated on foot, onland: the Semail, Josephine or Newfoundland ophiolites, for example, reveal important details on the genesis of oceanic lithosphere (*cf.* § 2; Tab. 1). We will see that ophiolites also preserve crucial information on the process of subduction initiation. The second type provides an essential glimpse onto the mechanisms of its destruction, i.e. on the subduction process itself: metamorphosed fragments keep traces of the transformations experienced at depth, during their transient burial and exhumation along the subduction plate boundary.

After briefly recalling some of the basic petrological features of the oceanic lithosphere (§ 2), this short odyssey starts by considering the relics left over by subduction and the precious insights they give us. Obduction is comparatively less frequent and in fact corresponds, as shown below, to one of subduction dead-ends.

2. Diversity of oceanic lithospheres

Two end-member types of oceanic lithosphere are recognized, depending on whether expansion rates and magmatic accretion are fast and profuse, or instead (ultra-)slow and limited (Fig. 2a). Pacific-type lithospheres belong to the first type, whereas the Atlantic, South-West Indian and Tethyan lithospheres exemplify the second one.

Fast-spreading oceans are characterized by a ~5-7 km thick and continuous crust made of gabbros and basalts (*'mafic' or basic rocks*), onto which a veneer of sediments is deposited, typically ~100 m thick far from subduction trenches (Clift and Vannucchi, 2004). This lithological structure is also referred to as the 'ocean plate stratigraphy' (Isozaki et al., 1990; Kusky et al., 2014; Wakabayashi et al., 2015). Magmatic production can increase significantly and the oceanic crust may reach up to ~20 km in oceanic plateaus (e.g., Ontong-Java, Aleutians).

At the other end of the spectrum, slow- and ultra-slow spreading oceans are heterogeneous, characterized by partly serpentinized mantle lithosphere intruded by gabbroic bodies exhumed to the seafloor through detachment faults (Cannat et al., 2006), and sparse magmatic segments or centers made of basalts and gabbros (Fig. 2a).

Oceanic lithosphere can thus be quite heterogeneous vertically or laterally, through variations of morphology, structure, lithology and crustal thickness. Another source of heterogeneity comes from the considerable variations of surface features and rugosity (Lallemand et al., 2018): seamounts and ridges – magmatic or not, as well as major fracture zones, transform faults or bending faults formed near subduction trenches (Ranero et al., 2003). These features can be very unevenly distributed, as observed along strike Chile for example (Fig. 2b).

3. Blueschists and eclogites: fragments that have escaped irreversible burial

Oceans vanish on geological timescales (Fig. 1). Fragments recovered from subduction depths, albeit precious to probe Earth's interiors, are very subordinate compared to the vast amounts of oceanic lithosphere metamorphosed and irreversibly subducted. The fate of oceanic lithosphere in subduction zones is illustrated in the following through two main examples: (1) a former seamount recently discovered in SW Iran, exposed in the Neotethyan suture within the Zagros orogen; (2) the extensively documented domain of the European Alps, with many well-preserved blueschists and eclogites.

3.1 Siah Kuh (Zagros, Iran): a seamount subducted at shallow depths and later exhumed

The oceanic origin of this massif, largely volcanic, is reflected in its architecture and petrology (Bonnet et al., 2019). From bottom to top, its succession comprises peridotites, gabbros, with typical oceanic textures; a >2 km-thick sequence of basalts capped by reef limestones and other sediments. Younger lava flows were emplaced on top of the sediments, revealing the existence of a prolonged magmatic activity (Fig. 3a-c). The sedimentary sequence reveals a progressive subsidence of this massif on the seafloor: shallow-water coral-bearing limestones, then slope deposits with limestone fragments and *débris-flows*, and finally deep-sea radiolarites. The dimensions of Siah Kuh, ~15 km*20 km and about 2 km high (its base is not exposed), appear comparable to seamounts observed on the seafloor (Fig. 2b; Cloos, 1992).

This massif, though largely intact, is made up of two distinct units (A and B) separated by a several kilometer-long thrust that exposes the mantle and gabbros of unit B (Fig. 3d). The massif is not only deformed but also shows mineral transformations that attest to its partial burial during subduction. Transformations are more pervasive in the northeast quarter of the edifice (Fig. 3c The presence of metamorphic aragonite, lawsonite or recrystallization of blue amphibole reveal subduction of the B unit to a pressure of 0.8 GPa (Bonnet et al., 2019; Figs. 3c,e). The Siah Kuh massif therefore consists of two adjacent portions of oceanic lithosphere subducted down to a maximum ~25-30 km depth, considering pressure estimates as lithostatic pressure, then scraped off the downgoing plate (i.e., the 'slab'). They were finally embedded in the Eurasian margin as a result of the collision between the Arabian and Eurasian plates during the Tertiary.

This nicely preserved seamount has therefore evolved and recrystallized at the seismogenic depths of subduction zones, where the largest seismic ruptures reach moment magnitudes Mw greater than 8 (i.e. hundred-kilometer-long ruptures, such as the 2010 Maule earthquake in Chile or the 2011 Tohoku earthquake in Japan; Figs. 1b, 3g). Evaluating seismic risk and

predicting the magnitude of (future) earthquakes requires assessing the mechanical behavior and along-strike segmentation of the subduction zone (Fig. 1b). Therefore, whether morphological and lithological heterogeneities entering the subduction trench (such as seamounts or seamount chains: Figs. 1b, 2b) constitute barriers to the propagation of earthquakes, and therefore control earthquake size, or instead form asperities likely to trigger them, is currently much debated (Wang and Bilek, 2014; Lallemand et al., 2018).

The Siah Kuh seamount suggests that stresses accumulated on this massif did not induce a major subduction earthquake. Pseudotachylites, which are considered as the most reliable evidence for the local and brief melting of rocks by the frictional heat released during an earthquake, are rare and their size would indicate magnitudes Mw less than 3 (Fig. 3g; Bonnet et al., 2019). If there were once major earthquakes, they carefully avoided the interior of Siah Kuh (Fig. 3g).

Subducted seamounts, although rarely preserved as intact, are found as fragments offscraped and later accreted to shallow depths in former accretionary prisms in Japan, California, Turkey or New Zealand. The Iranian example, however, compared to others, commonly hm– to km–scale at best, provides access to the entire structure in 3D. This example also provides an opportunity to study the deformation processes and mineral transformations at these depths, as well as the nature and pathways of fluids involved in the formation of veins and water-rich minerals (e.g., lawsonite).

3.2 The Alpine regional-scale record of subduction processes

In the heart of the Alps, the 'internal' domains preserve the trace of two extinct oceanic branches of the Alpine Ocean: the Liguro-Piemont and Valais domains (Figs. 4a,b; Lemoine et al., 1986; Vissers et al., 2013). The small, ~700 km wide Alpine Ocean can be compared to a rather narrow zone of today's North Atlantic Ocean, such as between Norway and Greenland. Like the Atlantic, its slow-spreading nature is attested by the type of peridotite, commonly partly refertilized and showing the full range of compositions between inherited sub-continental and asthenospheric mantle (Manatschal and Müntener, 2009; Picazo et al., 2016), the abundance of mantle compared to the crust, and the frequent presence of sediments deposited directly onto the mantle (e.g., ophicalcites; Lemoine et al., 1986; Beltrando et al., 2014).

The various oceanic relics (pillow lavas, ancient sediments, gabbros and mantle) are now transformed to blueschist and eclogite facies rocks (Figs. 4c-e, 5), evidencing subduction of the Alpine Ocean (Berger and Bousquet, 2008; Agard et al., 2009). In the metabasalts, the minerals constituting the characteristic associations of blueschists include blue amphibole associated with lawsonite or epidote, or garnet, and for the eclogites, garnet and sodium clinopyroxene of jadeitic nature (Fig. 5; Angiboust et al., 2009; Groppo et al., 2009). Metasediments show

mineralogical associations with ferro-magnesio carpholite, lawsonite, chloritoid or garnet, from blueschists to eclogites (Goffé and Chopin, 1986; Plunder et al., 2012). These minerals reflect thermodynamic re-equilibration at pressures ranging from 1-1.3 GPa at 300-400°C to 2.8-3.0 GPa at about 550-570°C, respectively (Fig. 6a; Agard, 2021). Considering that pressure estimates correspond to lithostatic pressure, these rocks indicate equivalent burial depths from approximately ~30 km down to 80-100 km.

Fragments of the upper few kilometers of the slab are found almost intact in places. In Monviso the mantle/gabbro/basalt/sediment sequence is overall preserved (Angiboust et al., 2011), although these rocks were likely buried at a depth of 80 km (Fig. 5g). Fracturing at peak burial is even found in some eclogites (e.g., eclogitic breccias; Fig. 5f), otherwise deformed in an intimate, ductile manner; they likely represent the scars of past subduction earthquakes (Angiboust et al., 2012; Locatelli et al., 2018).

The distribution of these alpine fragments reveals first order contrasts:

(1) Across the French-Italian Alps, the most intensely metamorphosed rocks are found in the eastern part of the Liguro-Piemont domain (Figs. 4c, 6b), indicating that the ocean subducted to the east, under Apulia (i.e. the present-day Po Plain). These rocks furthermore formed along a gradient of ~8-10°C/km typical of mature subduction zones, considering pressure as lithostatic (Agard et al., 2018; Fig. 6a).

(2) A much larger fraction of sediments (than mafic crust has been exhumed, mostly from pressures between 1.3 and 2.1 GPa (Agard, 2021). They form the S (sedimentary) units, commonly referred to as 'Schistes Lustrés' or 'Bündnerschiefer' (Fig. 4d).

(3) Mafic eclogites (metabasalts, metagabbros), mainly present in the western Alps, are closely associated with serpentinites in MUM (mafic and ultramafic) units structurally distinct from their former seafloor sedimentary cover (Fig. 4d). They reached higher pressures, mostly between 2.3 and 2.8 GPa (hence equivalent depths up to 80 km), late in the history of oceanic subduction, at the time continental subduction began (Fig. 6c): no older crustal fragments have survived. These remnants of oceanic lithosphere correspond to fragments formerly located at the edge of the continent: their burial ages are only slightly older (~5 Ma) than those at the edge of the continental margin (Fig. 6c), and the age of initial magmatic crystallization of these gabbros (and basalts) dates from the beginning of the history of expansion (~170-155 Ma; Fig. 6d), which places them well at the edge of the continent (Fig. 7a).

(4) Non-metamorphic fragments of oceanic lithosphere, sometimes called 'ophiolites', are found in the Chenaillet and Platta massifs (Figs. 5d, 6b). However, unlike ophiolites presented in the following (§ 4), their spatial extension is on the 1-10 km scale and they have no metamorphic sole. They were likely sliced off the slab at shallow depth and emplaced in the subduction prism, like the Marine Headlands sliver in California, which was sliced off at a maximum 8-10 km depth (and is now exposed at the northern end of the Golden Gate; Meneghini and Moore, 2007).

(5) While subduction lasted for about 60 Myr through slow, cm/year closure between ~100 and 40 Ma (Fig. 6c), no fragment buried during the first half of this period has come back to us (Fig. 6d): that part of the ocean entirely disappeared. During the second half of the subduction period, only a small fraction of metasediments was returned, and finally a few rare mafic eclogites at the end of oceanic subduction (Fig. 6d).

These fragments of oceanic lithosphere allow to reconstruct the history of subduction from a chronological and mechanical point of view (Figs. 7a,b). In detail, the spatial contrasts in type, abundance and burial of these fragments allow recognizing several sectors with distinct ocean subduction dynamics (sectors A to D; Fig. 7c). They reveal, in addition, that the imprint of oceanic convergence has deeply influenced today's collisional architecture and contrasts (Fig. 7c; Agard and Handy, 2021).

3.3 Lessons learnt from blueschists and eclogites

Oceanic fragments offscraped from the slab provide us with key samples to study their mineralogical, chemical and mechanical transformations. They give direct access to the composition, structure and rheology of rocks at the plate interface down to great depths, with a high spatial resolution inaccessible (yet) to geophysical observations. Since the subduction plate contact must transiently jump from the base of the upper plate to within the slab to detach slices from it (Figs. 3g, 7a), they shed light on mechanical coupling across the plate boundary.

Subducted oceanic fragments worldwide reveal that variations in interplate mechanical coupling (Agard et al., 2018) are statistically more frequent around equivalent depths of 30-40 km (at the base of the seismogenic zone; Menant et al., 2019) or 70-80 km (Fig. 8a). Beyond ~2.8 GPa, nothing is recovered: the eclogitized oceanic crust is significantly denser than the surrounding dry mantle (Agard et al., 2009, 2018) and is moreover dragged by the strong coupling established between the two plates beyond ~80 km (see § 4; Wada and Wang, 2009; van Keken et al., 2011). The size of the fragments and their pressure-temperature evolution through time suggest that the plate boundary is a few hundred meters thick at most (Agard et al., 2018; Wakabayashi, 2021; Figs. 8b,c), at odds with the results and/or assumptions of most numerical models. Fragments also appear dominantly derived from slow-spreading oceans (Agard, 2021), whose heterogeneous lithosphere and former detachment faults (Fig. 2a) make it easier to slice off fragments during subduction (Ruh et al., 2015). This is for example the case for the Alps and for the spectacular blueschists and eclogites of the Cyclades, a similarly restricted and once slow-spreading oceanic domain (Schmid et al., 2020; Gyomlai et al., 2021).

4. Fragments of oceanic lithosphere spared from subduction: ophiolites

4.1 The Semail ophiolite and beyond

Let's now turn to almost fully preserved fragments of oceanic lithosphere: ophiolites. The iconic Semail ophiolite straddles the northern part of Oman and the United Arab Emirates (Fig. 9a). Perfectly exposed in an arid environment, ~500 km long, ~100 km wide and locally 12-15 km thick, unaffected by any subsequent collision, it is by far the most studied in the world. It is regarded, since the Penrose conference of 1972, as representative of the Pacific type oceanic lithosphere. A mafic crust, composed from top to bottom of km-scale basaltic flows (Fig. 9c), a km-thick sheeted dyke complex and a few kilometers of gabbros (Fig. 9d), overlies mantle rocks that are dominantly depleted harzburgites (Fig. 9e). This succession is similar to that recognized in marine geophysics (2A, 2B , 3 and 4, respectively; Fig. 2a). Below the ophiolite, a distinctive hundred meter-thick metamorphic 'sole' is present, which comprises deformed and metamorphosed basalts and sediments (Figs. 9f,g). Further below, the continental crust exhibits blueschists and eclogites (Figs. 9h-j).

The Semail ophiolite has been scrutinized over the last 50 years to study the genesis of oceanic lithosphere (Coleman, 1981; Nicolas, 1989), revealing the existence of (mappable) mantle diapirs (Nicolas et al., 2000) or the interactions between ascending magmas and mantle rocks (Kelemen et al., 1995). The lessons learnt from the Semail ophiolite are of general relevance and pertain, with some variations, to other large ophiolitic massifs worldwide such as in New Caledonia, Newfoundland, Turkey, Cyprus, Timor or Papua New Guinea (Tab.1). While the exact geodynamic context in which the Semail ophiolite formed is still partly debated, most recent studies suggest that it formed around 95 Ma in a suprasubduction context (Rioux et al., 2012), i.e. right above an intra-oceanic subduction zone, and was then emplaced – 'obducted' – when it was a few million years old only (Agard et al., 2020 and references therein).

4.2 The obduction two-step process: triggering and ophiolite emplacement

Ophiolites attest that large, several hundred km-long pieces of oceanic lithosphere can be emplaced on top of continental lithosphere (Tab. 1; Fig. 10a). How can a dense, rigid and thin oceanic lithosphere be emplaced on top of a continental lithosphere with the exact opposite characteristics: light, deformable and thick (Fig. 10b)? Superimposing lithospheres requires lithospheric-scale shortening, which hints to subduction initiation. This provides a simple answer: if intraoceanic subduction is initiated close to the continental margin, yet dipping away from the continent (Fig. 10c), the margin may in turn be subducted below the adjacent oceanic

lithosphere, i.e. below the future ophiolite (e.g., Searle et al., 2004; Agard et al., 2007; Edwards et al., 2015). In this case, ophiolites are the witnesses of an intra-oceanic subduction that has turned to a dead end, stopped by the subduction of a continental margin (or of an island arc: e.g., Josephine ophiolite). Docking of the 'Cordilleran' ophiolites (Moores, 1982) is more enigmatic, but also relates to intraoceanic subduction dynamics (Wakabayashi and Dilek, 2003; Agard et al., 2020, their Fig. 3a).

In the case of the Semail ophiolite, why was a new subduction zone initiated near the Arabian margin since one already existed to the north, beneath Eurasia (Figs. 10c,d)? The Semail obduction followed an episode of major plate kinematics reorganization around 110 ± 5 Ma, marked by a sharp increase in convergence velocity between Arabia and Eurasia (Agard et al., 2007), the opening of the Atlantic Ocean and the formation of large mantle plumes in the eastern Pacific (Vaughan and Scarrow, 2003) and in the Indian Ocean (Rodriguez et al., 2021). Onset of subduction to the south of the Neotethys (Fig. 10c; at ~104 Ma: Guilmette et al., 2018) indicates that the preexisting subduction zone to the north was unable to accommodate the entire convergence between Arabia and Eurasia (Agard et al., 2007). Similar perturbations also predated the obduction of most ophiolites whose geodynamic context can still be reconstructed (e.g., Turkey, Timor, New Caledonia).

The scenario, from the abyssal plain to the exposure of the ophiolite, can be reconstructed quite precisely in the case of Semail, thanks to the metamorphic and sedimentary record (Figs. 9g,j). Two crucial stages of the obduction process are preferentially preserved: (i) its start, which shows the (difficult) initiation of intraoceanic subduction (§ 4.3); (ii) its termination, which results in the effective emplacement of the (rather passive) ophiolite by subduction, or 'underthrusting', of the continental lithosphere (§ 4.4).

4.3 Obduction birth: onset of intraoceanic subduction and slab dynamics ('slabitization')

The fragments located immediately below the ophiolite represent our best witnesses, so far, of intra-oceanic subduction initiation (Figs. 11a,b). Immediately below the ophiolite, the metamorphic sole exposes extremely deformed material constituting the top of an oceanic lithosphere (Gnos, 1998; Figs. 9f,g): metabasalts and metamorphosed pelagic sediments, in particular former radiolarites. This reveals that some oceanic crust was underplated below oceanic lithosphere, thereby demonstrating the existence of intra-oceanic subduction (Wakabayashi and Dilek, 2000; Figs. 9c, 11a).

Metamorphic soles furthermore testify to the initial mechanical resistance to subduction (Figs. 11b,c). The sequence of rocks encountered in the sole (Fig. 9g) attests to the progressive

offscraping of the newly forming slab (Figs. 11a-d). This is reminiscent of the accidental offscraping observed for Siah Kuh or for blueschists and eclogites worldwide (§ 3), yet happens during the birth of subduction. The internal organization of the metamorphic sole allows drawing major inferences: (1) the stripping of the slab first affects the entire crust (basalts, and sometimes the sheeted dyke complex) then is confined to the most superficial levels, the sediments (Fig. 11d); (2) the formation and progressive accretion of the sole involves materials that are less and less metamorphic with time (HT then LT: Figs. 9g, 11d): first granulite- then amphibolite- and finally greenschist-facies rocks, revealing a general cooling of the system at the same time as a more and more pellicular offscraping of the slab (Soret et al., 2017, 2019). This process ceases with the gradual cooling of the subduction and the lubrication of the new interface between the plates, in part due to the serpentinization of the mantle of the upper plate (Agard et al., 2016; Fig. 11e).

The base of the mantle is made up of 'low temperature' foliated peridotites (Figs. 9e,g; Ceuleneer et al., 1988; Prigent et al., 2018a). These portions of the ophiolite are characterized by a very intense deformation, distributed over a thickness of a kilometer or so, which is similar to that of the underlying metamorphic sole (Fig. 11b): synchronous, in the same direction and in the same temperature range decreasing with time (from ~900 to 650°C, around 1 GPa). With time, deformation gets more and more localized near the contact with the metamorphic sole. Geochemical data show that this deformation is accompanied by the percolation of slab-derived fluids into the ophiolite base (travelling at meters per year; Prigent et al., 2018b), which represents an essential witness of element transfer during subduction (Fig. 11f; in comparison, no intact interplate interface is preserved in the mature subduction environments probed by blueschists and eclogites).

The mechanical coupling between the metamorphic sole and the foliated peridotites records the very early stages of the disappearance of the oceanic lithosphere (Fig. 11e), while subduction is still in its infancy (Agard et al., 2016). Deformation is first distributed over a characteristic thickness exceeding one kilometer before deformation gets localized along a mature, 1-100 m thick plate contact (stages 1-3, Fig. 11e).

As the subduction thermal structure cools and the new slab progresses downward, the zone of strong mechanical resistance/coupling between the plates deepens (black dot, Fig. 11f): this process, coined as 'slabitization' (Agard et al., 2020), unzips the subduction plate interface down to a depth referred to as the common depth of viscous coupling (CDVC, ~80 km depth; Wada and Wang, 2009). The onset of mechanical coupling gradually initiates a mantle counterflow and leads, through decompression and fluid ingression, to mantle melting and embryonic arc magmatism (with forearc basalts, boninites; Stern and Bloomer, 1992; Ishizuka et al., 2020; Fig. 11f). This explains the formation of the Semail ophiolite in a supra-subduction context (and of many others: Tab. 1). After a few million years, once mechanical coupling has stabilized at the

CDVC (Fig. 11f), hydrated melting appears and generates the classical subduction-related andesitic magmas (Fig. 1; Stern, 2002; Bonnet et al., 2020).

As a result of this evolution, the subduction interface has become mechanically decoupled in the long term down to a depth of about 100 km (Fig. 11e-f): slab fragments will not be recovered except during mechanical and/or geodynamic perturbations able to trigger the offscraping of blueschists and eclogites (§ 3; Agard et al., 2018). This process also explains the close relationship between subduction initiation and the genesis (and future emplacement) of the ophiolite, and their close ages. In the case of Semail, the whole process lasts about 10 Myr (Figs. 11a,f): transformation and burial of the metamorphic soles range from 105-100 to 95 Ma (Rioux et al., 2016; Guilmette et al., 2018), while the ophiolite has yielded a narrow age range, around 96-95 Ma (Rioux et al., 2012). More fundamentally, the processes of subduction initiation and 'slabitization' accompany the birth of a new slab, before it becomes connected to and starts interacting with the convecting asthenospheric mantle.

In most cases, preserved ophiolites correspond to 'fresh' oceanic lithosphere newly formed in a supra-subduction setting (Table 1). There are, however, less common examples of ophiolites that correspond to tracts of oceanic lithosphere formed well before any convergence started (e.g., Armenia, Sistan; Table 1; Agard et al., 2020, their Fig. 3b). This indicates that intraoceanic subduction was unable to drive mantle upwelling, probably as a result of shorter-lived subduction (those examples also show cooler metamorphic soles; Agard et al., 2020).

4.4 Obduction death: ophiolites preserved through continental subduction

Unmetamorphosed pelagic sediments are found below the base of the Semail ophiolite and its metamorphic sole (Hawasina units; Figs. 9b, 10a), as for the Bay of Island or Lycian ophiolites (Tab. 1). These were scraped off during the underthrusting of the distal part of the continental margin. Even lower, in the Saih Hatat and Jabal Akhdar tectonic windows, blueschist and eclogite facies metamorphic rocks crop out (Figs. 9b,h-j,10a). These fragments are again witnesses of a subduction process, but this time that of continent subduction (Goffé et al., 1984; as for the Briançonnais domain in the Alps; § 3, Figs. 5,7). These portions of the Arabian continental margin are easily recognizable through their Permian to Late Cretaceous sedimentary successions and their Proterozoic metasediments already metamorphosed during the ~600-550 Ma Panafrican orogeny (Béchennec et al., 1989; Cozzi et al., 2012; Fig. 10a). The rocks from the Saih Hatat window were dragged into subduction, reaching variable pressures from 1 to 2.3 GPa (Yamato et al., 2007; Massonne et al., 2013).

Peak burial of these continental rocks occurred around 80 Ma. Their exhumation is marked by spectacular ductile deformation, including km-scale sheath folds (Searle and Alsop, 2007;

Scharf et al., 2021). Here again, preservation was selective: while the burial history is partially fossilized in minerals (Yamato et al., 2007), the macroscopic structures associated with burial have been largely erased, and only the exhumation dynamics can be restored (Fig. 12a; Yamato et al., 2007; Agard et al., 2010). The large folds and intense shearing accompanying exhumation of these rocks attest that they must have moved upwards, likely along the subduction interface, during or following the choking of the subduction zone (Searle et al., 2004). Continental subduction was transient (Agard and Vitale-Brovarone, 2013), the low density and greater thickness of the continental margin preventing long-lived subduction (Fig. 12b; like sponge below chocolate in figure 10b...). All convergence had disappeared by 75-70 Ma.

The entire obduction crisis therefore lasted about 25 Myr (Fig. 12a), as for obduction events elsewhere (cf. New Caledonia: Cluzel et al., 2001; Soret et al., 2016; Vitale-Brovarone et al., 2018; Timor: Linthout et al., 1997). In essence, what ultimately allows for the effective emplacement of the ophiolite and its good preservation (thanks also to the absence of later collision, as opposed to the ophiolite fragments scattered in the Himalayan/Tibet sutures; Fig. 1c), is continental subduction.

Obduction is therefore both an accident and a subduction dead end. At the plate tectonics scale, it can be seen as the result of a change in the partitioning of deformation between the different convergence zones (Figs. 10c,d; Agard et al., 2014). Thermomechanical geodynamic models allow testing the obduction scenario quantitatively by estimating the theoretical P-T-t paths of the rocks and characteristic duration of the process (Fig. 12b; Duretz et al., 2016; Porkolab et al., 2021). To a first approximation, the agreement between predictions and nature is satisfactory (Fig. 12c), notwithstanding the fact that extension is somewhat imposed in the model (i.e., subduction 'choking' is not produced self-consistently by the model), the 'spontaneous' formation of supra-subduction lithosphere is not accounted for and the role of 3D variations is not considered.

In fact, the case of the Semail ophiolite reveals the important impact of crustal heterogeneities and lateral contrasts within the continental margin on the final structure of the ophiolite (as also observed in New Caledonia; Cluzel et al., 2001). The two tectonic windows below the ophiolite, the Saih Hatat (to the east) and Jebel Akhdar windows (to the west), evidence first-order differences (Fig. 13a). In the Saih Hatat, rocks were subducted down much higher pressure and exhumation is characterized by major shearing and deformation; this sector of the continental margin was also cut across by mafic intrusions during the Permian rifting of the Neotethys (Chauvet et al., 2009). On the contrary, the Jebel Akhdar, which is devoid of mafic intrusions of Permian age, only reached a peak pressure of ~0.7 GPa (Breton, 2004; hence, in terms of

equivalent depths, not much more than the 10-15 km-thick ophiolite above) and experienced only moderate obduction-related deformation.

Large contrasts are also observed offshore, in the Gulf of Oman (Figs. 13b-c). The Jebel Akhdar transect reveals the existence of a major ~80 Ma thrust affecting the offshore part of the Semail ophiolite and of a strongly subsiding sedimentary basin, with profuse infill and debris-flows (olistostrome in Fig. 13b) dated from the Campanian (i.e. 80-75 Ma; Ninkabou et al., 2021). The Saih Hatat transect, on the contrary, is marked by pronounced Maastrichtian uplift and Maastrichtian to lower Tertiary extension and exposes continental material below the ophiolite (Fig. 13c). These onshore and offshore contrasts are observed across the Semail Gap (Fig. 13a), a major fault zone considered to be inherited from the Pan-African orogeny (Cozzi et al., 2012; Scharf et al., 2019). They are comparable in scale to those observed in the subducted continental margin of the Alps (Fig. 7; Agard, 2021).

Worthy of note, the structure of the ophiolite shows comparatively limited lateral contrasts (whether petrological or paleomagnetic; Nicolas et al., 2000; van Hinsbergen et al., 2019), except for the larger supra-subduction imprint west of the Semail Gap (Python et al., 2008). This shows that the late exhumation of the Saih Hatat blueschists and eclogites occurred without deforming much the ophiolite above, suggesting that the tectonic contact in between them was then rheologically rather weak. Importantly, the very limited syn-convergence sedimentary record of obduction (restricted to the west of the Semail Gap) suggests that most of the obduction-related shortening proceeded without significant erosion, hence presumably underwater.

5. The fate of oceanic lithosphere: tragic yet insightful

Blueschists, eclogites and ophiolites are all that remain of ancient oceanic lithosphere. They are precious relics allowing to probe depths inaccessible to direct observation and to study the onset of plate tectonics on Earth (Moores, 2002). These fragments of oceanic lithosphere provide us with unique information on the mechanical behaviour of rocks, which is essential to understand seismic risks, or on the transfer of fluids and elements, which is crucial to understand volcanic processes or elemental recycling within the globe.

This overview shows the intimate links and the differences between subduction and obduction processes. It allows distinguishing true ophiolites (constitutive of the upper plate) from fragments of oceanic lithosphere offscraped from the downgoing slab (Fig. 14a-b), whether these were deeply subducted or only shallowly accreted to the upper plate. It also underlines the importance of the evolution of the subduction regime through time (Figs. 11e, 14c-f).

What blueschists and eclogites record are the dynamics of mature subduction zones, the

mechanics of the subduction plate interface... and its hiccups. Ophiolites and their metamorphic soles as well, but at the time of subduction initiation and with complementary insights. Both types of relics even give us a kind of wink: the initiation of subduction is enlightened by obduction, while subduction proves to be essential to obduction. Yet, as for any historical landmark, they are primarily accidents: they reveal transient episodes in the otherwise rather smooth, well-established subduction process, which dooms oceans to disappear.

Acknowledgements:
Immense thanks are due to S. Angiboust, M. Locatelli, B. Dubacq, S. Guillot, M. Handy, J. Wakabayashi, A. Vitale-Brovarone, T. Duretz, M. Jentzer and many others, for fruitful and friendly discussions over the years.

Reference list

Agard, P., Jolivet, L., Vrielynck, B., Burov, E., & Monie, P. (2007). Plate acceleration: The obduction trigger? *Earth and Planetary Science Letters*, *258*(3–4), 428–441. https://doi.org/10.1016/j.epsl.2007.04.002

Agard, P., Yamato, P., Jolivet, L., & Burov, E. (2009). Exhumation of oceanic blueschists and eclogites in subduction zones: Timing and mechanisms. *Earth-Science Reviews*, *92*(1–2), 53–79. https://doi.org/10.1016/j.earscirev.2008.11.002

Agard, P., Omrani, J., Jolivet, L., Whitechurch, H., Vrielynck, B., Spakman, W., et al. (2011). Zagros orogeny: a subduction-dominated process. *Geological Magazine*, *148*(5–6), 692–725. https://doi.org/10.1017/S001675681100046X

Agard, P., Yamato, P., Soret, M., Prigent, C., Guillot, S., Plunder, A., et al. (2016). Plate interface rheological switches during subduction infancy: Control on slab penetration and metamorphic sole formation. *Earth and Planetary Science Letters*, *451*, 208–220. https://doi.org/10.1016/j.epsl.2016.06.054

Agard, P., Plunder, A., Angiboust, S., Bonnet, G., & Ruh, J. (2018). The subduction plate interface: rock record and mechanical coupling (from long to short timescales). *Lithos*, *320–321*, 537–566. https://doi.org/10.1016/j.lithos.2018.09.029

Agard, P. (2021). Subduction of oceanic lithosphere in the Alps: Selective and archetypal from (slow-spreading) oceans. *Earth-Science Reviews*, 103517.

Agard, P., & Handy, M. R. (2021). Ocean subduction dynamics in the Alps. *Elements: An International Magazine of Mineralogy, Geochemistry, and Petrology*, *17*(1), 9–16.

Agard, P., & Vitale-Brovarone, A. (2013). Thermal regime of continental subduction: the record from exhumed HP–LT terranes (New Caledonia, Oman, Corsica). *Tectonophysics*, *601*, 206–215.

Agard, P., Searle, M. P., Alsop, G. I., & Dubacq, B. (2010). Crustal stacking and expulsion tectonics during continental subduction: P-T deformation constraints from Oman. *Tectonics*, *29*(5).

Agard, P., Zuo, X., Funiciello, F., Bellahsen, N., Faccenna, C., & Savva, D. (2014). Obduction: Why, how and where. Clues from analog models. *Earth and Planetary Science Letters*, *393*, 132–145.

Agard, P., Prigent, C., Soret, M., Dubacq, B., Guillot, S., & Deldicque, D. (2020). Slabitization: Mechanisms controlling subduction development and viscous coupling. *Earth-Science Reviews*, *208*, 103259.

Angiboust, S., Agard, P., Jolivet, L., & Beyssac, O. (2009). The Zermatt-Saas ophiolite: the largest (60-km wide) and deepest (c. 70-80 km) continuous slice of oceanic lithosphere detached from a subduction zone? *Terra Nova*, *21*(3), 171–180. https://doi.org/10.1111/j.1365-3121.2009.00870.x

Angiboust, S., Agard, P., Raimbourg, H., Yamato, P., & Huet, B. (2011). Subduction interface processes recorded by eclogite-facies shear zones (Monviso, W. Alps). *Lithos*, *127*(1–2), 222–238. https://doi.org/10.1016/j.lithos.2011.09.004

Angiboust, S., Agard, P., Yamato, P., & Raimbourg, H. (2012). Eclogite breccias in a subducted ophiolite: A record of intermediate-depth earthquakes? *Geology*, *40*(8), 707–710. https://doi.org/10.1130/G32925.1

Béchennec, F., Le Metour, J., Rabu, D., Beurrier, M., Bourdillon-Jeudy-de-Grissac, C., De Wever, P., et al. (1989). Geologie d'une chaine issue de la Tethys; les montagnes d'Oman. *Bulletin de La Société Géologique de France*, (2), 167–188.

Beltrando, M., Manatschal, G., Mohn, G., Dal Piaz, G. V., Brovarone, A. V., & Masini, E. (2014). Recognizing remnants of magma-poor rifted margins in high-pressure orogenic belts: The Alpine case study. *Earth-Science Reviews*, *131*, 88–115.

Berger, A., & Bousquet, R. (2008). Subduction-related metamorphism in the Alps: review of isotopic ages based on petrology and their geodynamic consequences. *Geological Society, London, Special Publications*, *298*(1), 117–144.

Bonnet, G., Agard, P., Angiboust, S., Fournier, M., & Omrani, J. (2019). No large earthquakes in fully exposed

subducted seamount. *Geology*, *47*(5), 407–410.
Bonnet, G., Agard, P., Whitechurch, H., Fournier, M., Angiboust, S., Caron, B., & Omrani, J. (2020a). Fossil seamount in southeast Zagros records intraoceanic arc to back-arc transition: New constraints for the evolution of the Neotethys. *Gondwana Research*, *81*, 423–444.
Bonnet, G., Agard, P., Whitechurch, H., Fournier, M., Angiboust, S., Caron, B., & Omrani, J. (2020b). Fossil seamount in southeast Zagros records intraoceanic arc to back-arc transition: New constraints for the evolution of the Neotethys. *Gondwana Research*, *81*, 423–444.
Brovarone, A. V., Agard, P., Monie, P., Chauvet, A., & Rabaute, A. (2018). Tectonic and metamorphic architecture of the HP belt of New Caledonia. *Earth-Science Reviews*, *178*, 48–67.
Ceuleneer, G., Nicolas, A., & Boudier, F. (1988). Mantle flow patterns at an oceanic spreading centre: the Oman peridotites record. *Tectonophysics*, *151*(1–4), 1–26.
Chauvet, F., Dumont, T., & Basile, C. (2009). Structures and timing of Permian rifting in the central Oman Mountains (Saih Hatat). *Tectonophysics*, *475*(3–4), 563–574.
Clift, P., & Vannucchi, P. (2018). Controls on tectonic accretion versus erosion in subduction zones: Implications for the origin and recycling of the continental crust. *Reviews of Geophysics*, *42*(2). https://doi.org/10.1029/2003RG000127
Cloos, M. (1992). Thrust-Type Subduction-Zone Earthquakes and Seamount Asperities - a Physical Model for Seismic Rupture. *Geology*, *20*(7), 601–604. https://doi.org/10.1130/0091-7613(1992)020<0601:TTSZEA>2.3.CO;2
Cluzel, D., Aitchison, J. C., & Picard, C. (2001). Tectonic accretion and underplating of mafic terranes in the Late Eocene intraoceanic fore-arc of New Caledonia (Southwest Pacific): geodynamic implications. *Tectonophysics*, *340*(1–2), 23–59.
Coleman, R. G. (1971). Plate tectonic emplacement of upper mantle peridotites along continental edges. *Journal of Geophysical Research*, *76*(5), 1212–1222.
Coleman, Robert G. (1981). Tectonic setting for ophiolite obduction in Oman. *Journal of Geophysical Research: Solid Earth*, *86*(B4), 2497–2508.
Coltice, N., Gérault, M., & Ulvrová, M. (2017). A mantle convection perspective on global tectonics. *Earth-Science Reviews*, *165*, 120–150.
Dewey, J. F. (1976). Ophiolite obduction. *Tectonophysics*, *31*(1–2), 93–120.
Duretz, T., Agard, P., Yamato, P., Ducassou, C., Burov, E. B., & Gerya, T. V. (2016). Thermo-mechanical modeling of the obduction process based on the Oman ophiolite case. *Gondwana Research*, *32*, 1–10.
Ernst, W. (1971). Metamorphic zonations on presumably subducted lithospheric plates from Japan, California and the Alps. *Contributions to Mineralogy and Petrology*, *34*(1), 43–59.
Forsyth, D., & Uyeda, S. (1975). On the relative importance of the driving forces of plate motion. *Geophysical Journal International*, *43*(1), 163–200.
Gnos, E. (1998). Peak metamorphic conditions of garnet amphibolites beneath the Semail Ophiolite: Implications for an inverted pressure gradient. *International Geology Review*, *40*(4), 281–304. https://doi.org/10.1080/00206819809465210
Goffe, B., & Chopin, C. (1986). High-pressure metamorphism in the Western Alps: zoneography of metapelites, chronology and consequences. *Schweizerische Mineralogische Und Petrographische Mitteilungen*, *66*(1–2), 41–52.
Goffé, B., Michard, A., Kienast, J. R., & Le Mer, O. (1988). A case of obduction-related high-pressure, low-temperature metamorphism in upper crustal nappes, Arabian continental margin, Oman: PT paths and kinematic interpretation. *Tectonophysics*, *151*(1–4), 363–386.
Groppo, C., Beltrando, M., & Compagnoni, R. (2009). The P–T path of the ultra-high pressure Lago di Cignana and adjoining high-pressure meta-ophiolitic units: insights into the evolution of the subducting Tethyan slab. *Journal of Metamorphic Geology*, *27*(3), 207–231.
Guilmette, C., Smit, M. A., van Hinsbergen, D. J., Gürer, D., Corfu, F., Charette, B., et al. (2018). Forced subduction initiation recorded in the sole and crust of the Semail Ophiolite of Oman. *Nature Geoscience*, *11*(9), 688–695.
Gyomlai, T., Agard, P., Marschall, H. R., Jolivet, L., & Gerdes, A. (2021). Metasomatism and deformation of block-in-matrix structures in Syros: The role of inheritance and fluid-rock interactions along the subduction interface. *Lithos*, *386*, 105996.
Ishizuka, O., Taylor, R. N., Umino, S., & Kanayama, K. (2020). Geochemical evolution of arc and slab following subduction initiation: a record from the Bonin Islands, Japan. *Journal of Petrology*.
Isozaki, Y., Maruyama, S., & Furuoka, F. (1990). Accreted oceanic materials in Japan. *Tectonophysics*, *181*(1–4), 179–205.
Kaneko, Y., Maruyama, S., Kadarusman, A., Ota, T., Ishikawa, M., Tsujimori, T., et al. (2007). On-going orogeny in the outer-arc of the Timor–Tanimbar region, eastern Indonesia. *Gondwana Research*, *11*(1–2), 218–233.
Kelemen, P. B., Shimizu, N., & Salters, V. J. (1995). Extraction of mid-ocean-ridge basalt from the upwelling mantle by focused flow of melt in dunite channels. *Nature*, *375*(6534), 747–753.
Kusky, T. M., Windley, B. F., Safonova, I., Wakita, K., Wakabayashi, J., Polat, A., & Santosh, M. (2013). Recognition of ocean plate stratigraphy in accretionary orogens through Earth history: A record of 3.8billion years of sea floor spreading, subduction, and accretion. *Gondwana Research*, *24*(2), 501–547. https://doi.org/10.1016/j.gr.2013.01.004
Lallemand, S., Peyret, M., van Rijsingen, E., Arcay, D., & Heuret, A. (2018a). Roughness characteristics of oceanic seafloor prior to subduction in relation to the seismogenic potential of subduction zones. *Geochemistry, Geophysics, Geosystems*, *19*(7), 2121–2146.

Lallemand, S., Peyret, M., van Rijsingen, E., Arcay, D., & Heuret, A. (2018b). Roughness characteristics of oceanic seafloor prior to subduction in relation to the seismogenic potential of subduction zones. *Geochemistry, Geophysics, Geosystems*, *19*(7), 2121–2146.

Lemoine, M., Bas, T., Arnaud-Vanneau, A., Arnaud, H., Dumont, T., Gidon, M., et al. (1986). The continental margin of the Mesozoic Tethys in the Western Alps. *Marine and Petroleum Geology*, *3*(3), 179–199.

Linthout, K., Helmers, H., & Sopaheluwakan, J. (1997). Late Miocene obduction and microplate migration around the southern Banda Sea and the closure of the Indonesian Seaway. *Tectonophysics*, *281*(1–2), 17–30.

Locatelli, M., Verlaguet, A., Agard, P., Federico, L., & Angiboust, S. (2018). Intermediate-depth brecciation along the subduction plate interface (Monviso eclogite, W. Alps). *Lithos*, *320*, 378–402.

Manatschal, G., & Müntener, O. (2009). A type sequence across an ancient magma-poor ocean–continent transition: the example of the western Alpine Tethys ophiolites. *Tectonophysics*, *473*(1–2), 4–19.

Massonne, H.-J., Opitz, J., Theye, T., & Nasir, S. (2013). Evolution of a very deeply subducted metasediment from As Sifah, northeastern coast of Oman. *Lithos*, *156*, 171–185.

Menant, A., Angiboust, S., & Gerya, T. (2019). Stress-driven fluid flow controls long-term megathrust strength and deep accretionary dynamics. *Scientific Reports*, *9*(1), 1–11.

Meneghini, F., & Moore, J. C. (2007). Deformation and hydrofracture in a subduction thrust at seismogenic depths: The Rodeo Cove thrust zone, Marin Headlands, California. *Geological Society of America Bulletin*, *119*(1–2), 174–183. https://doi.org/10.1130/B25807.1

Moores, E. M. (1982). Origin and emplacement of ophiolites. *Reviews of Geophysics*, *20*(4), 735–760.

Moores, Eldridge M. (2002). Pre–1 Ga (pre-Rodinian) ophiolites: Their tectonic and environmental implications. *Geological Society of America Bulletin*, *114*(1), 80–95.

Nicolas, A. (1989). Structures of ophiolites and dynamics of oceanic lithosphere. *Structures of Ophiolites and Dynamics of Oceanic Lithosphere*. Retrieved from https://www.scopus.com/inward/record.uri?eid=2-s2.0-85040886915&partnerID=40&md5=17b50b83cc6eca46fb5331ec22375966

Nicolas, A., Boudier, F., Ildefonse, B., & Ball, E. (2000). Accretion of Oman and United Arab Emirates ophiolite–discussion of a new structural map. *Marine Geophysical Researches*, *21*(3–4), 147–180.

Ninkabou, D., Agard, P., Nielsen, C., Smit, J., Gorini, C., Rodriguez, M., et al. (2021). Structure of the offshore obducted Oman margin: emplacement of Semail ophiolite and role of tectonic inheritance. *Journal of Geophysical Research: Solid Earth*, *126*(2), 2020JB020187.

Pearce, J. A., & Robinson, P. (2010). The Troodos ophiolitic complex probably formed in a subduction initiation, slab edge setting. *Gondwana Research*, *18*(1), 60–81.

Picazo, S., Müntener, O., Manatschal, G., Bauville, A., Karner, G., & Johnson, C. (2016). Mapping the nature of mantle domains in Western and Central Europe based on clinopyroxene and spinel chemistry: Evidence for mantle modification during an extensional cycle. *Lithos*, *266*, 233–263.

Plunder, A., Agard, P., Dubacq, B., Chopin, C., & Bellanger, M. (2012). How continuous and precise is the record of P-T paths? Insights from combined thermobarometry and thermodynamic modelling into subduction dynamics (Schistes Lustres, W. Alps). *Journal of Metamorphic Geology*, *30*(3), 323–346. https://doi.org/10.1111/j.1525-1314.2011.00969.x

Porkoláb, K., Duretz, T., Yamato, P., Auzemery, A., & Willingshofer, E. (2021). Extrusion of subducted crust explains the emplacement of far-travelled ophiolites. *Nature Communications*, *12*(1), 1–11.

Prigent, C., Guillot, S., Agard, P., Lemarchand, D., Soret, M., & Ulrich, M. (2018). Transfer of subduction fluids into the deforming mantle wedge during nascent subduction: Evidence from trace elements and boron isotopes (Semail ophiolite, Oman). *Earth and Planetary Science Letters*, *484*, 213–228. https://doi.org/10.1016/j.epsl.2017.12.008

Prigent, Cécile, Agard, P., Guillot, S., Godard, M., & Dubacq, B. (2018). Mantle Wedge (De) formation During Subduction Infancy: Evidence from the Base of the Semail Ophiolitic Mantle. *Journal of Petrology*, *59*(11), 2061–2092.

Python, M., Ceuleneer, G., & Arai, S. (2008). Chromian spinels in mafic–ultramafic mantle dykes: evidence for a two-stage melt production during the evolution of the Oman ophiolite. *Lithos*, *106*(1–2), 137–154.

Ranero, C. R., Morgan, J. P., McIntosh, K., & Reichert, C. (2003). Bending-related faulting and mantle serpentinization at the Middle America trench. *Nature*, *425*(6956), 367–373. https://doi.org/10.1038/nature01961

Rioux, M., Bowring, S., Kelemen, P., Gordon, S., Dudás, F., & Miller, R. (2012). Rapid crustal accretion and magma assimilation in the Oman-UAE ophiolite: High precision U-Pb zircon geochronology of the gabbroic crust. *Journal of Geophysical Research: Solid Earth*, *117*(B7).

Rioux, M., Garber, J., Bauer, A., Bowring, S., Searle, M., Kelemen, P., & Hacker, B. (2016). Synchronous formation of the metamorphic sole and igneous crust of the Semail ophiolite: New constraints on the tectonic evolution during ophiolite formation from high-precision U–Pb zircon geochronology. *Earth and Planetary Science Letters*, *451*, 185–195.

Rodriguez, M., Arnould, M., Coltice, N., & Soret, M. (2021). Long-term evolution of a plume-induced subduction in the Neotethys realm. *Earth and Planetary Science Letters*, *561*, 116798.

Ruh, J. B., Le Pourhiet, L., Agard, P., Burov, E., & Gerya, T. (2015). Tectonic slicing of subducting oceanic crust along plate interfaces: Numerical modeling. *Geochemistry, Geophysics, Geosystems*, *16*(10), 3505–3531.

de Saussure, H. B. (1804). *Voyages dans les Alpes: précédés d'un essai sur l'histoire naturelle des environs de Genève* (Vol. 2). L. Fauche-Borel, imprimeur.

Scharf, A, Mattern, F., Moraetis, D., Callegari, I., & Weidle, C. (2019). Postobductional kinematic evolution and geomorphology of a major regional structure—The Semail Gap Fault Zone (Oman Mountains). *Tectonics*, *38*(8), 2756–2778.

Scharf, Andreas, Mattern, F., Al-Wardi, M., Frijia, G., Moraetis, D., Pracejus, B., et al. (2021). Tectonic evolution of the Oman Mountains. *Geological Society, London, Memoirs*, *54*(1), 67–103.

Schmid, S. M., Fügenschuh, B., Kounov, A., Maţenco, L., Nievergelt, P., Oberhänsli, R., et al. (2020). Tectonic units of the Alpine collision zone between Eastern Alps and western Turkey. *Gondwana Research*, *78*, 308–374.

Searle, M., & Alsop, G. (2007). Eye-to-eye with a mega–sheath fold: A case study from Wadi Mayh, northern Oman Mountains. *Geology*, *35*(11), 1043–1046.

Soret, M., Agard, P., Ildefonse, B., Dubacq, B., Prigent, C., & Rosenberg, C. (2019). Deformation mechanisms in mafic amphibolites and granulites: record from the Semail metamorphic sole during subduction infancy. *Solid Earth Discussions*, *2019*, 1–36. https://doi.org/10.5194/se-2019-28

Soret, Mathieu, Agard, P., Dubacq, B., Vitale-Brovarone, A., Monie, P., Chauvet, A., et al. (2016). Strain localization and fluid infiltration in the mantle wedge during subduction initiation: Evidence from the base of the New Caledonia ophiolite. *Lithos*, *244*, 1–19.

Soret, Mathieu, Agard, P., Dubacq, B., Plunder, A., & Yamato, P. (2017). Petrological evidence for stepwise accretion of metamorphic soles during subduction infancy (Semail ophiolite, Oman and UAE). *Journal of Metamorphic Geology*, *35*(9), 1051–1080. https://doi.org/10.1111/jmg.12267

Stern, R. J. (2002). Subduction zones. *Reviews of Geophysics*, *40*(4), 3–1.

Stern, R. J., & Bloomer, S. H. (1992). Subduction zone infancy: examples from the Eocene Izu-Bonin-Mariana and Jurassic California arcs. *Geological Society of America Bulletin*, *104*(12), 1621–1636.

Van Hinsbergen, D. J., Maffione, M., Koornneef, L. M., & Guilmette, C. (2019). Kinematic and paleomagnetic restoration of the Semail ophiolite (Oman) reveals subduction initiation along an ancient Neotethyan fracture zone. *Earth and Planetary Science Letters*, *518*, 183–196.

Van Keken, P. E., Hacker, B. R., Syracuse, E. M., & Abers, G. A. (2011). Subduction factory: 4. Depth-dependent flux of H2O from subducting slabs worldwide. *Journal of Geophysical Research: Solid Earth*, *116*(B1).

Wada, I., & Wang, K. (2018). Common depth of slab-mantle decoupling: Reconciling diversity and uniformity of subduction zones. *Geochemistry, Geophysics, Geosystems*, *10*(10). https://doi.org/10.1029/2009GC002570

Wakabayashi, J., & Dilek, Y. (2000). Spatial and temporal relationships between ophiolites and their metamorphic soles: A test of models of forearc ophiolite genesis. In Y. Dilek, E. M. Moores, D. Elthon, & A. Nicolas (Eds.), *Ophiolites and Oceanic Crust: New Insights from Field Studies and Ocean Drilling Program* (pp. 53–64). Boulder: Geological Soc Amer Inc.

Wakabayashi, John. (2015). Anatomy of a subduction complex: architecture of the Franciscan Complex, California, at multiple length and time scales. *International Geology Review*, *57*(5–8), 669–746. https://doi.org/10.1080/00206814.2014.998728

Wakabayashi, J. (2021). Subduction and exhumation slip accommodation at depths of 10–80 km inferred from field geology of exhumed rocks: Evidence for temporal-spatial localization of slip. *Plate Tectonics, Ophiolites, and Societal Significance of Geology: A Celebration of the Career of Eldridge Moores*, *552*, 257.

Wang, K., & Bilek, S. L. (2011). Do subducting seamounts generate or stop large earthquakes? *Geology*, *39*(9), 819–822.

Warren, J. M. (2016). Global variations in abyssal peridotite compositions. *Lithos*, *248*, 193–219.

Yamato, P., Agard, P., Goffé, B., De Andrade, V., Vidal, O., & Jolivet, L. (2007). New, high-precision P–T estimates for Oman blueschists: implications for obduction, nappe stacking and exhumation processes. *Journal of Metamorphic Geology*, *25*(6), 657–682.

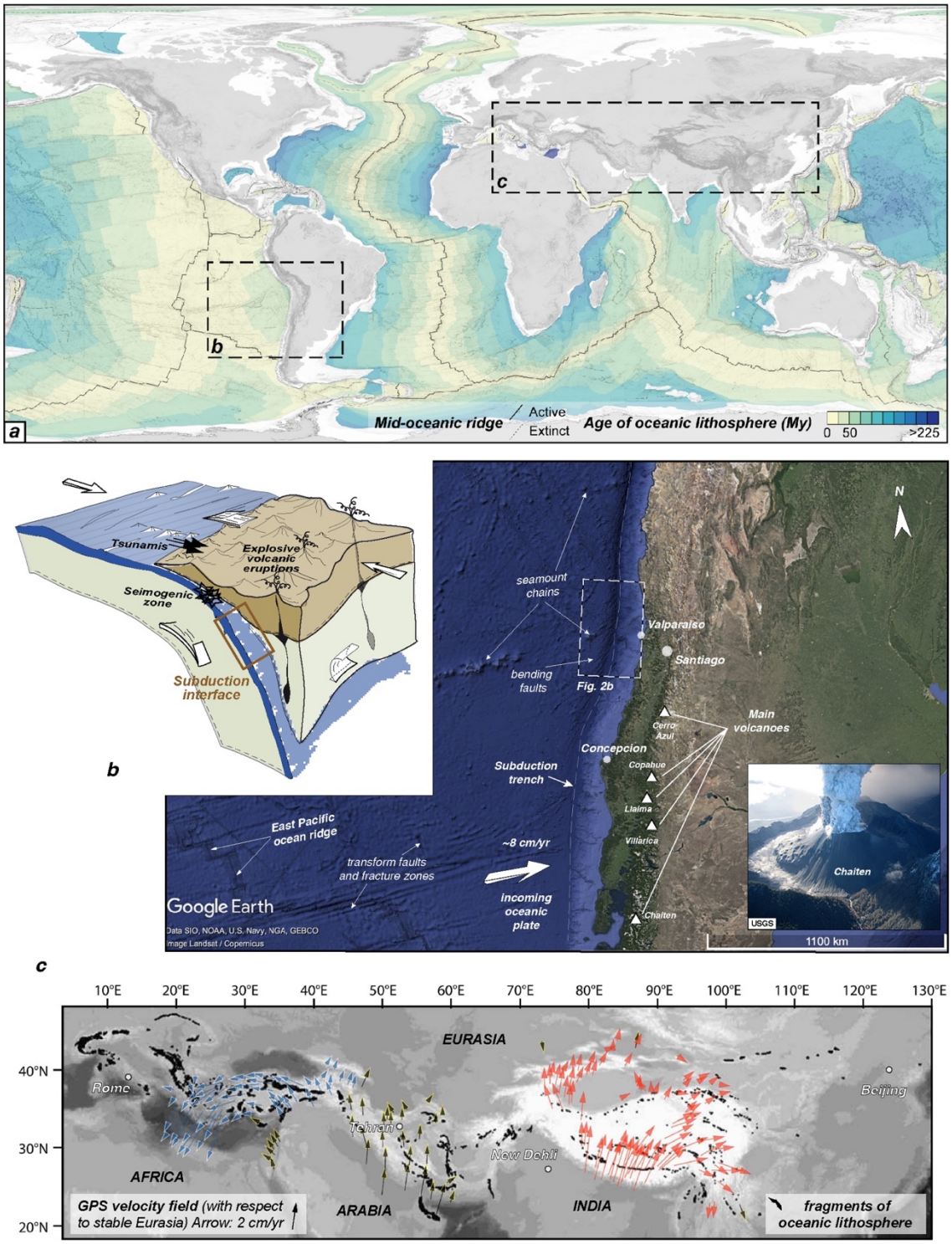

Fig. 1. *a) Age map of present-day oceanic lithosphere, after Seton et al. (2020). Almost all of it is younger than 200 Ma (save, perhaps, for parts of the eastern Mediterranean domain whose age is debated).*
b) The subduction process, where oceanic lithosphere goes down the "escalator", with devastating earthquakes triggered along the subduction interface, tsunamis and explosive volcanic eruptions. About half of the entire seismic energy of the globe is being released in the Chilean subduction zone!
c) The fragments of oceanic lithosphere disseminated along the 'suture zones' of the Alpine-Himalayan mountain belts mark the location of former Tethyan oceans. Arrows indicate present-day displacements, with respect to stable Eurasia, deduced from satellite data (after Agard et al., 2011).

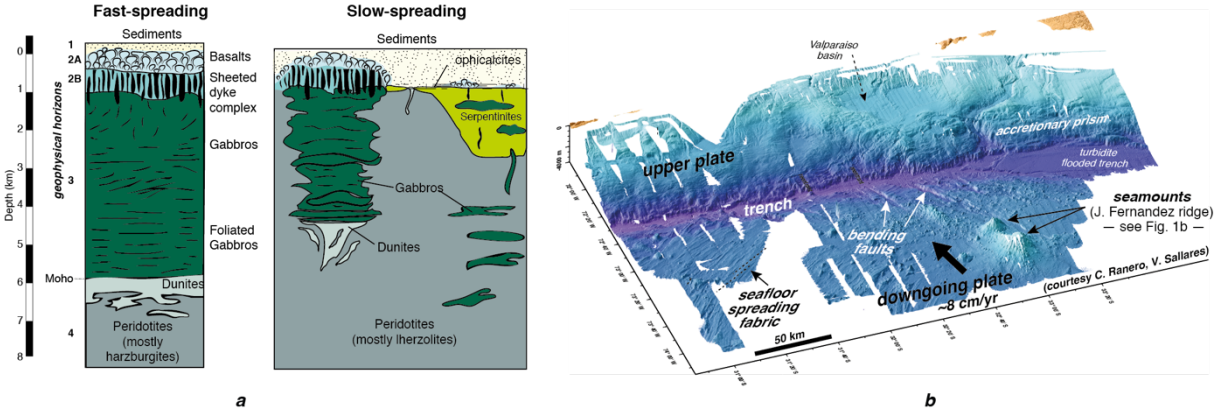

Fig. 2. *a) First-order characteristics of oceanic lithosphere formed at fast- (left) or slow-spreading oceans (right). b) Seafloor heterogeneities are remarkable: fractures zones, bending and transform faults, ocean ridges and seamounts, as shown here off Santiago, Chile (location on Fig. 1b).*

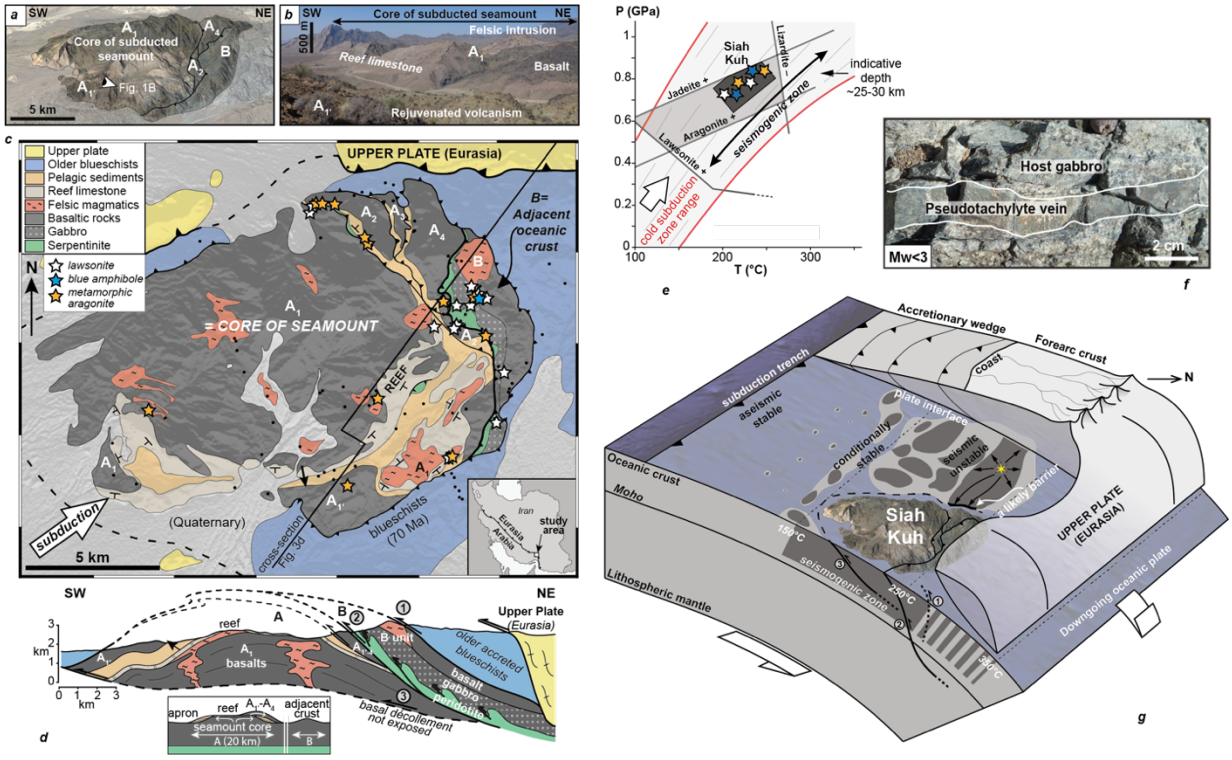

Fig. 3. *a) A former seamount stands out of the Quaternary infill, SW Iran: the Siah Kuh massif ('black mountain').*
b) Reef limestones form like a crown around the main volcanic edifice.
c) Simplified geological map of the massif outlining the main edifice (unit A) and the one to the NE (unit B), as well as the many mineral metamorphic recrystallisations, particularly in the vicinity of the large thrust separating units A and B.
d) Cross-section view showing the juxtaposition of the two portions of oceanic lithosphere and tentative restoration before offscraping along the subduction interface.
e) The stability of metamorphic minerals yields pressure estimates around 0.8 GPa for unit B. The greater extent of mineral transformations in the NE suggests a greater burial for the B unit, consistent with the former subduction direction to the NE, beneath Eurasia.
f) Only few pseudotachylites veins are observed in the Siah Kuh massif.
g) Idealized view of the Siah Kuh seamount at peak burial conditions, within the seismogenic zone.

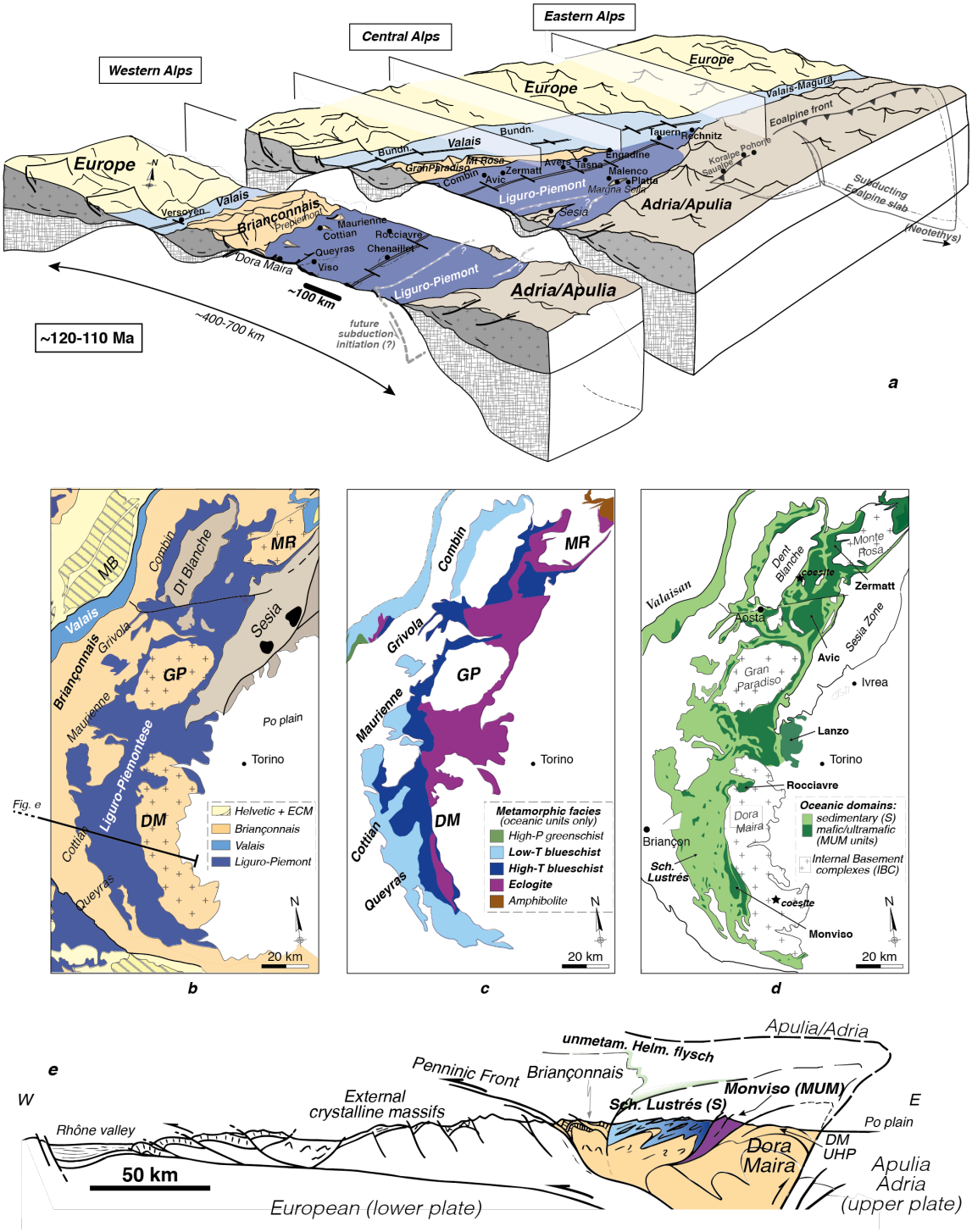

Fig. 4. *a) Schematic paleogeography of the Alpine ocean around 120 Ma, approximately at the time of its greatest extension (Agard, 2021). Some localities are indicated for reference.*
b) Structural sketch map of the Western Alps. Color coding is the same as for Fig. 4a and highlights, for example, the presence of an intervening continental block (the Briançonnais) between and along most of the Liguro-Piemont and Valais branches of the ocean.
c) Distribution of metamorphic facies along the Western Alps, showing a marked increase towards the east.
d) Distribution of lithologies along the Western Alps: note the spatial contrast, somewhat coincident with that of metamorphic facies, between the S (dominantly sedimentary) and MUM (dominantly mafic and ultramafic) units.
e) Crustal-scale section across the Western Alps, at the latitude of Monviso and Dora Maira (Fig. 4b). Remnants of the oceanic lithosphere include (i) the unmetamorphosed Helminthoid Flysch deposits (Helm. flysch) representing the former trench infill (see Fig. 7a), the dominantly sedimentary Schistes Lustrés and the mafic and ultramafic bodies like Monviso.

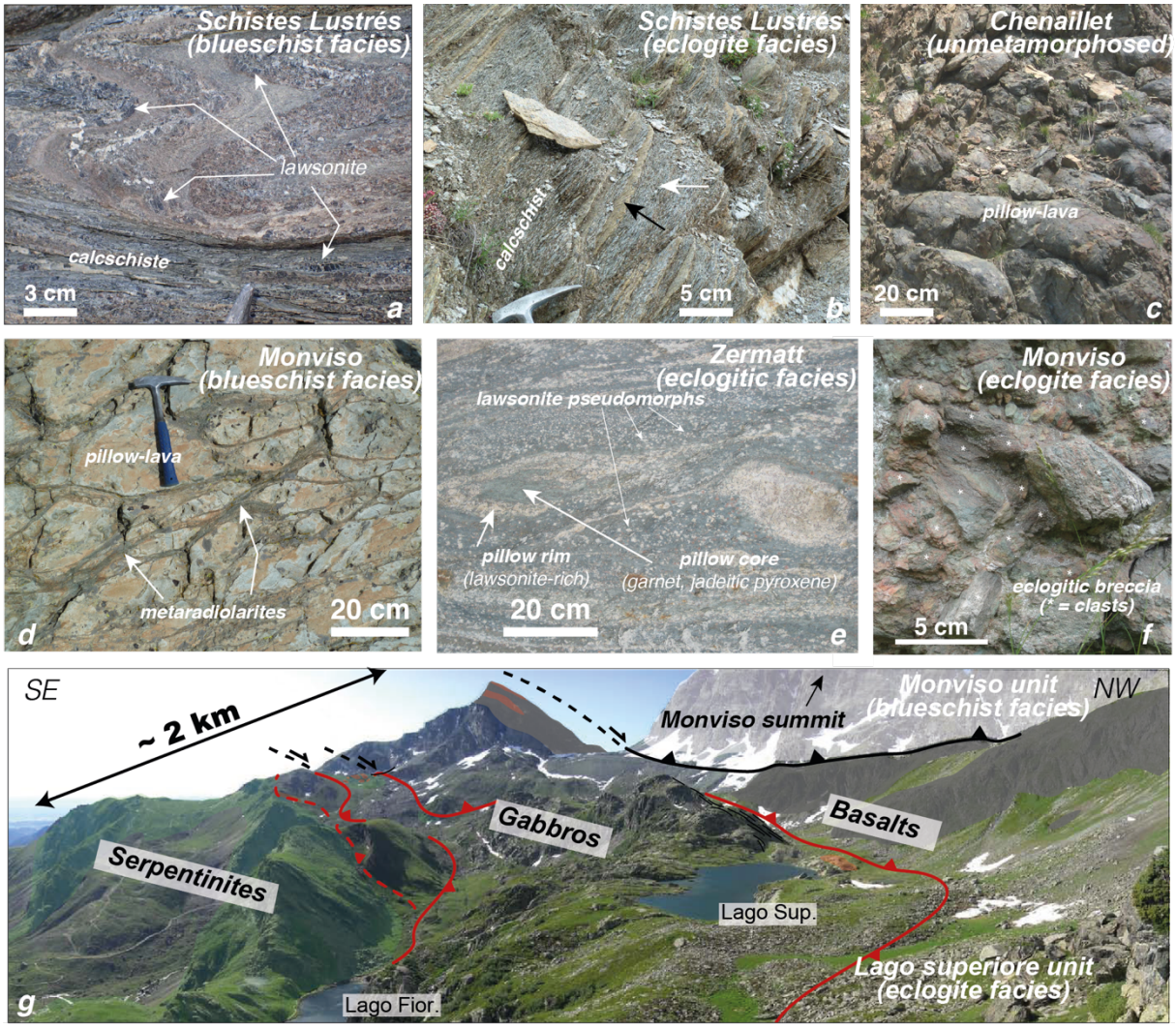

Fig. 5.
a-b) typical calschists of the Schistes Lustrés. Note the abundant lawsonite crystals in b (dark because of inclusions of organic matter); the black arrow in c underlines a more calcareous horizon in the dominantly pelitic metasediment (white arrow).
c-e) Former pillow-lavas from the Alpine oceanic crust now either unmetamorphosed (d), blueschist facies (e) or eclogite facies (f).
f) Metagabbros brecciated at eclogite facies conditions: the same eclogitic mineralogy is found in the clasts (underlined by stars) and in the cement.
g) One of the best-preserved pieces of slab in the world, and one of the deepest known so far: the Lago Superiore eclogitic tectonic slice (italian side of Monviso). See Angiboust et al. (2012) and Locatelli et al. (2018) for details.

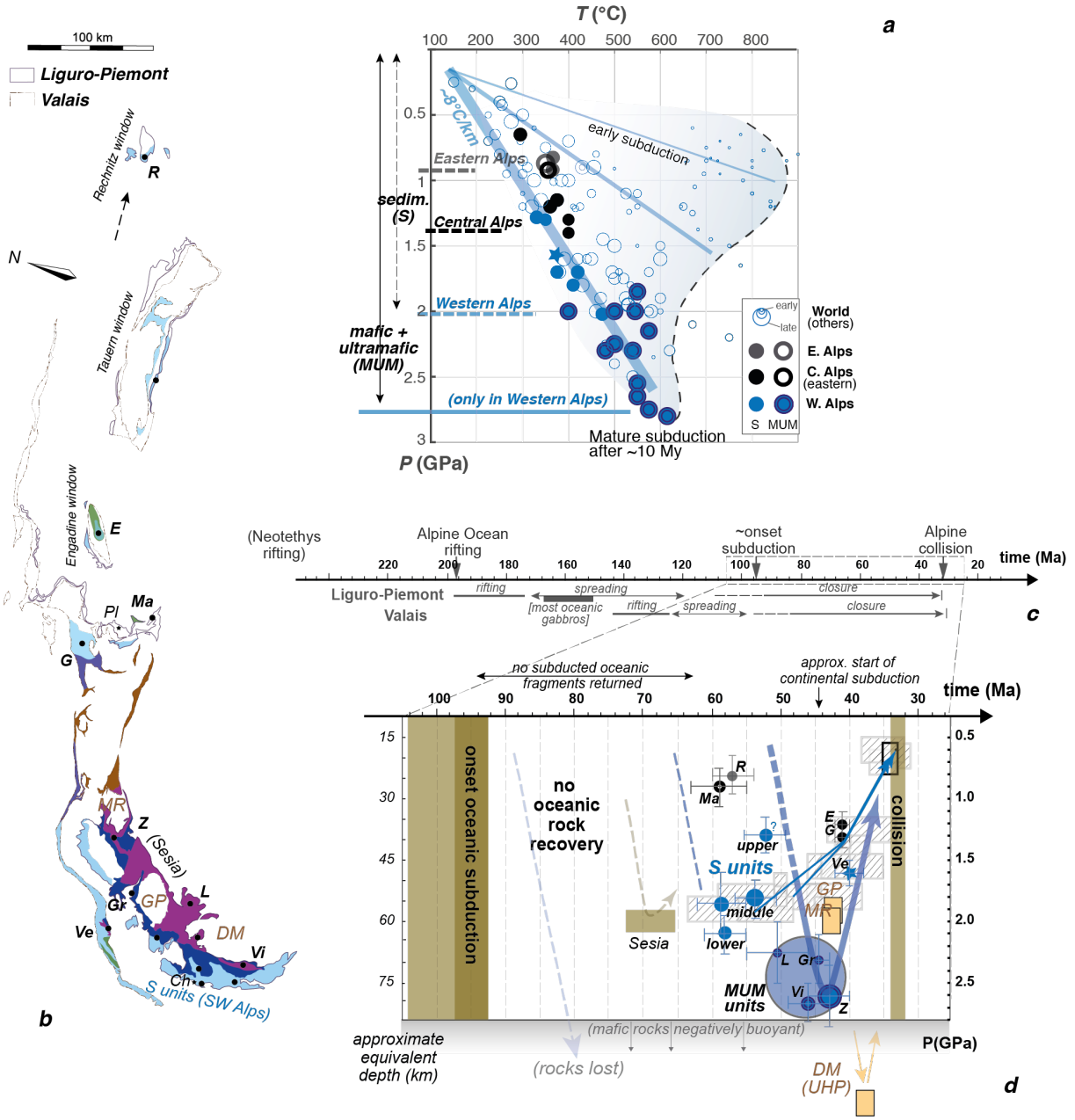

Fig. 6. *a) Maximum pressure (and burial) reached by representative subducted fragments from across the entire Alps (see Agard, 2021). Note the decrease of peak pressure towards the east, and the alignment of all remnants on the P-T gradient typical of mature subduction (hence suggesting ~8°C/km considering pressure as lithostatic). These estimates are set back against worldwide literature data (Agard et al., 2018).*
b) Map of the exposed remnants of oceanic lithosphere in the Alps. Metamorphosed oceanic fragments are color-coded as in Fig. 4c. Abbreviations: E: Engadine; G: Grisons; Gr: Grivola; L: Lanzo; Ma: Malenco; R: Rechnitz; Ve: Versoyen; Vi: Monviso. Some largely unmetamorphosed oceanic fragments are also found, like Chenaillet (Ch) or Platta (Pl). Large, eclogitized subducted continental fragments, in addition to Sesia, include Dora Maira (DM), Gran Paradiso (GP) and Monte Rosa (MR).
c) Opening and closure of the two branches of the Alpine ocean. Oceanic subduction lasted approximately 50-60 Myr.
d) Pressure-time paths of subducted fragments of oceanic lithosphere.

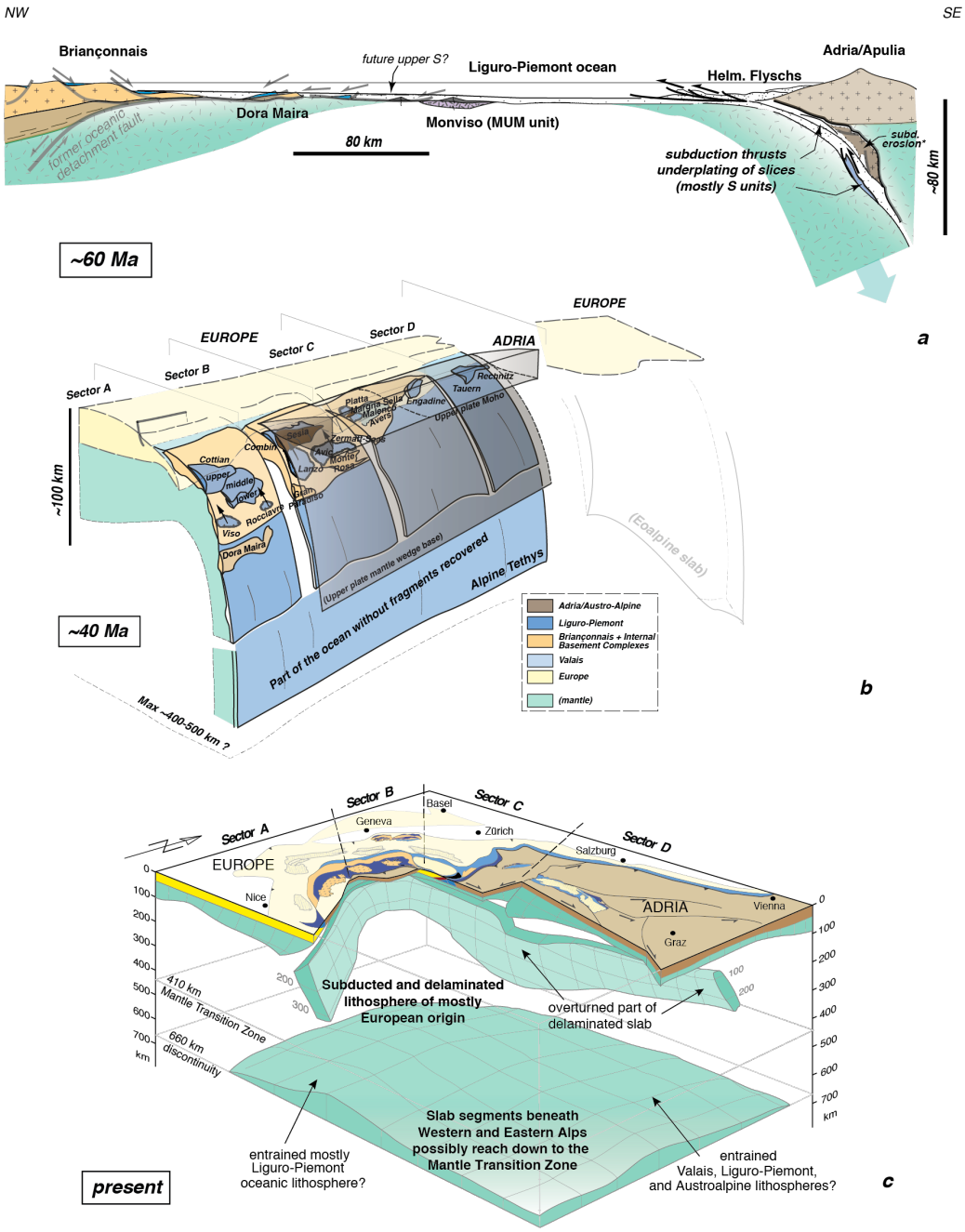

Fig. 7. *a) Restoration of the Liguro-Piemont subduction zone at ~60 Ma (Agard, 2021), showing that some metasedimentary units from the slab were offscraped during subduction. Recovered MUM units, like in Monviso, were subducted later and saved from irreversible burial into the mantle, partly thanks to continental subduction (Fig. 6c).*
b) Schematic 3D view, from the western to the eastern Alps of all oceanic units recovered from subduction Agard, 2021: petrological and lithological contrasts reveal the existence of distinct sectors with distinct subduction dynamics. This lateral segmentation was likely controlled, at least in part, by structures inherited from the former Variscan and/or rifting events.
c) Tomographic imaging outlining slab fragments recognized beneath the Alps (Agard and Handy, 2021; courtesy M. Handy and collaborators). Lateral contrasts seem to match those deduced from contrasts in oceanic subduction dynamics recognized independently. The entire oceanic lithosphere now lies in the Mantle Transition Zone, between 440 and 670 km depth.

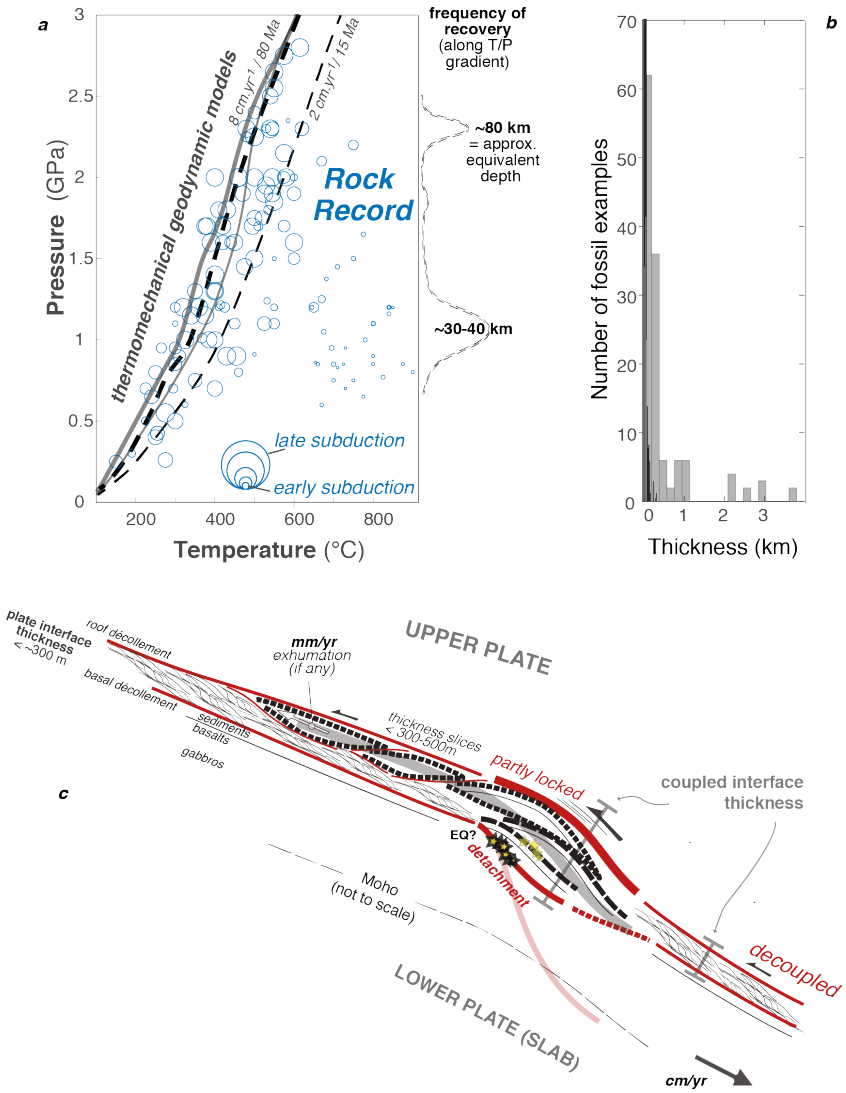

Fig. 8. *Geological and dynamic constraints on the plate interface (see Agard et al., 2018 for details). a) The subduction rock record is shown as a function of its relative timing of recovery in a given subduction history (e.g., early or late). It can be compared to the results of thermomechanical models for mature subduction. Rock recovery, though transient and relatively rare, is favoured at depths of 30-40 and 70-80 km (assuming P as lithostatic pressure).*
b) The thickness of the various tectonic slices allows placing constraints on the thickness of the plate interface and variations in mechanical coupling.
c) Integrated view of the subduction interface: thickness, composition, structure and mechanical behavior.

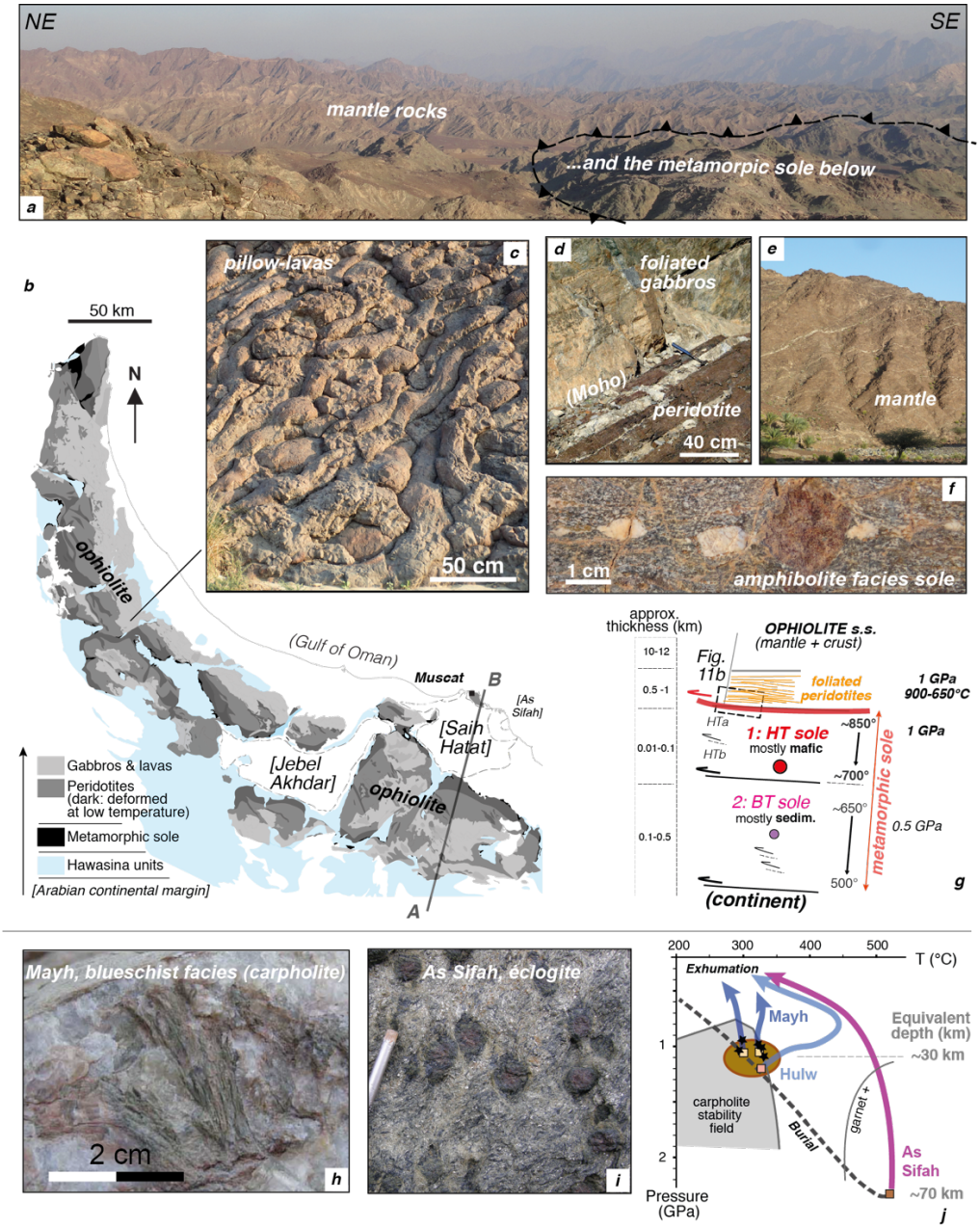

Fig. 9. *a) Mantle rocks peaking above the continental margin of Arabia over vast distances (across several hundreds of kilometers!) with a systematic though thin metamorphic sole plastered beneath it.*
b) Simplified tectonic map of north-eastern Oman and the UAE. The Semail ophiolite (grey colors) is overlying the Hawasina units (light blue), i.e. pelagic sediments deposited on the ocean floor and on the transitional domain between the continent and the Neotethys ocean. Structurally below is the continental lithosphere, with basement and recent sedimentary rocks nicely exposed in the Saih Hatat and Jabal Akhdar tectonic windows.
Blueschists and eclogites crop out in the former, whereas the latter shows more modest mineral transformations.
c-e) Typical horizons within the ophiolite: the famous pillow-lavas from Wadi Jizi (c), the Moho transition zone (d; courtesy C. Nicollet) and the variably deformed peridotites (e).
f) Close-up view on the metamorphic sole: here a former basal transformed to a (amphibolite- to granulite-facies) garnet-amphibole-plagioclase ± clinopyroxene rock.
g) Structural organization at the base of the ophiolite, showing the genetic association between the strongly foliated peridotites and the metamorphic sole (particularly the HT type).
h-i) Carpholite-bearing blueschist and eclogite with garnet and clinopyroxene relics (in a matrix of epidote, blue amphibole and white mica) from the Saih Hatat window.
j) P-T trajectories followed by the HP-LT metamorphic rocks of the Saih Hatat units (Figs. h,i) during exhumation.

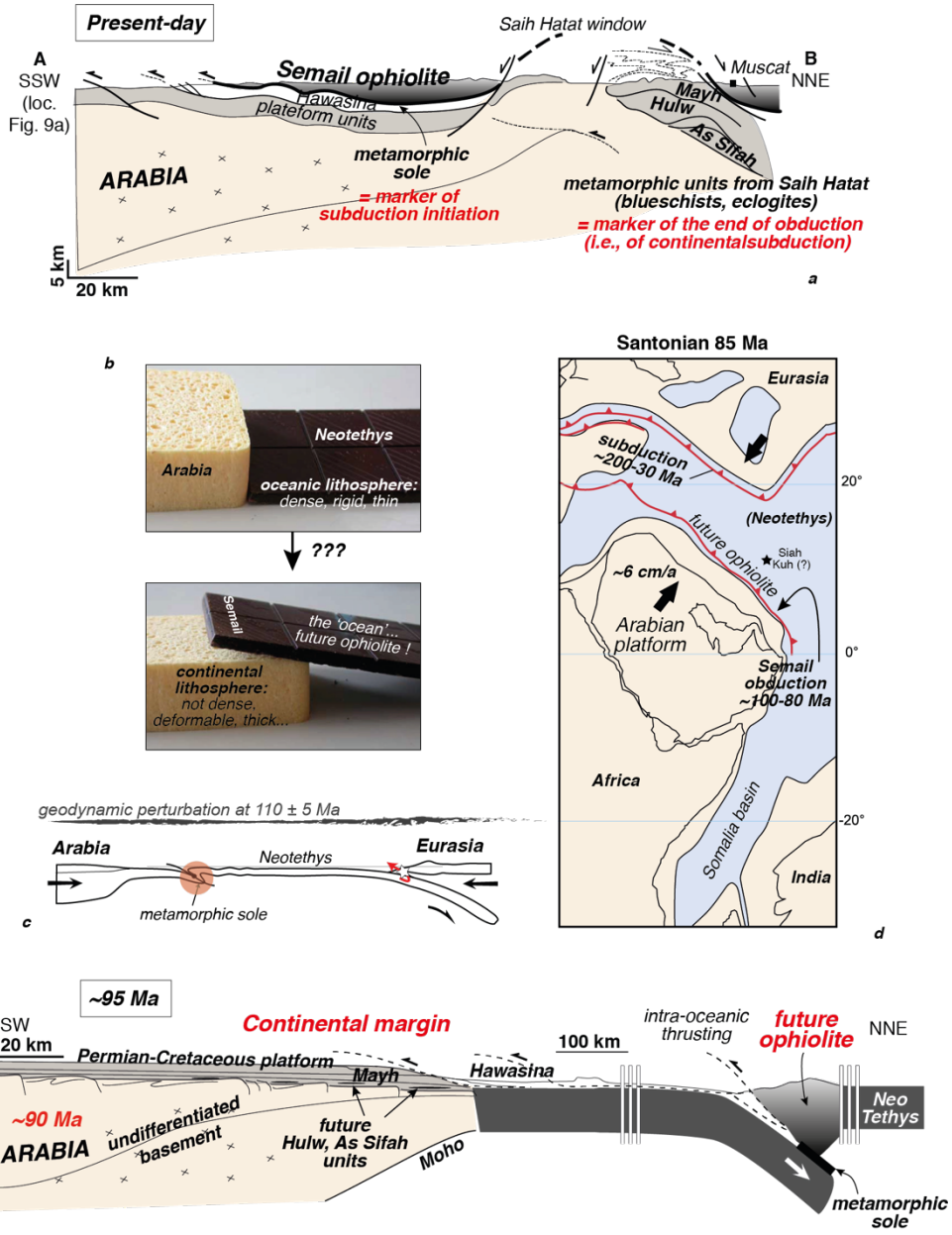

Fig. 10. *a) Present-day section across north-eastern Oman, with emphasis on the metamorphic landmarks of the start and end of the obduction history.*
b) How can oceanic lithosphere be emplaced on top of continental lithosphere?...
c) Onset of intra-oceanic subduction at the southern end of the Neotethys following Cretaceous kinematic reorganization (Agard et al., 2007; Matthews et al., 2012).
d) Late Cretaceous (85 Ma) paleogeography of the Arabia-Eurasia region (after Fournier et al., 2006) showing the disappearance of the Neotethys beneath Eurasia. This ocean had been subducting since ~200 Ma and was therefore much larger than the Alpine one (Fig. 4). The approximate location of the Siah Kuh seamount is indicated here (see § 3.1; Bonnet et al., 2020).
e) Restoration of the northern margin of Arabia at 100-95 Ma (simplified after Béchennec et al., 1989 ; Searle et al., 2004). Comparing figures a and e allows capturing the emplacement of the Semail ophiolite: first through intra-oceanic subduction and then underthrusting of the continental margin beneath the ophiolite.

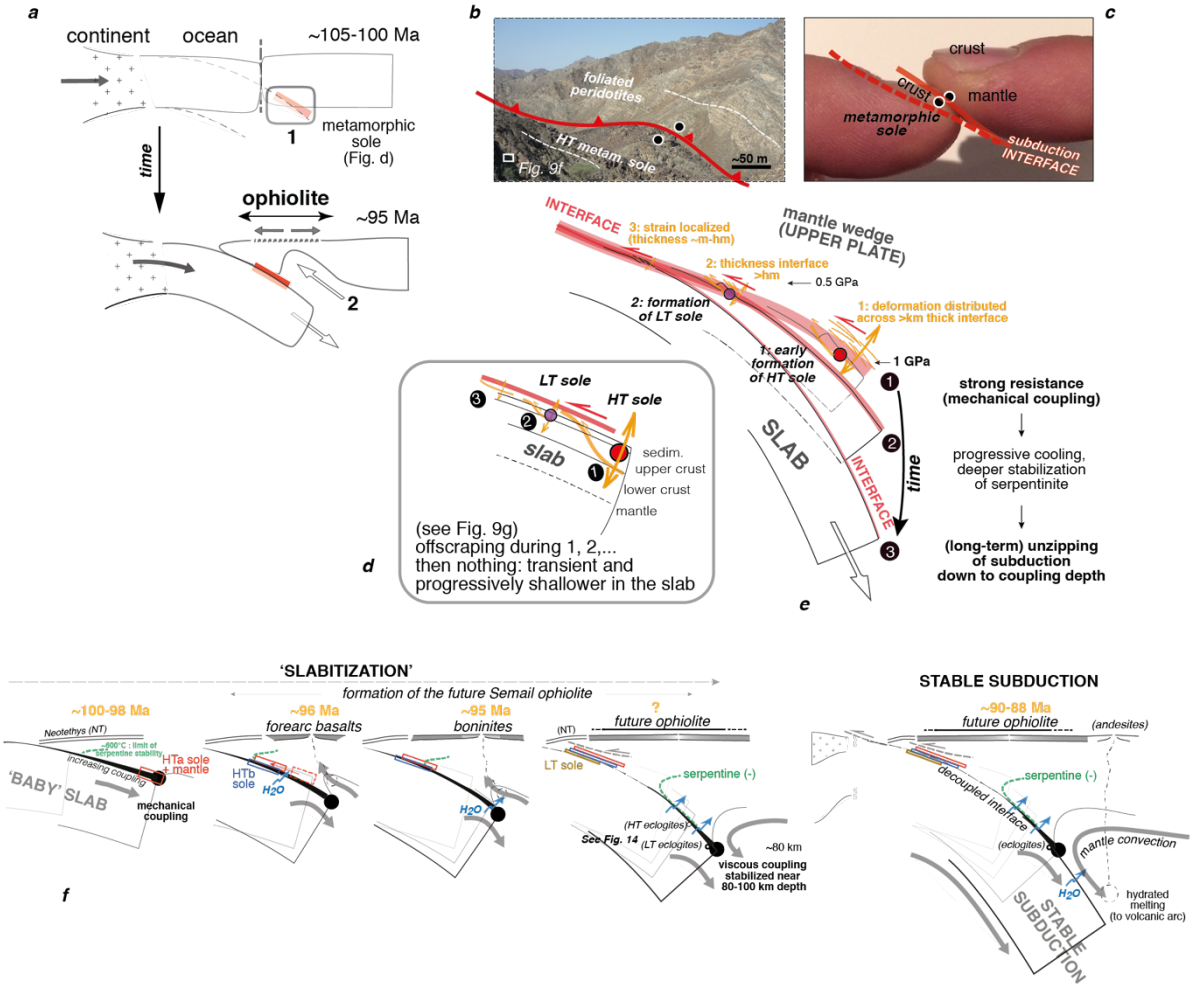

Fig. 11. *a) Simple tectonic evolution outlining the genetic link between intra-oceanic subduction and obduction. The start of oceanic subduction is systematically accompanied by the stripping of fragments of oceanic crust (the future metamorphic sole) from incipiently sinking oceanic lithosphere (the future slab). The obducted ophiolite, in our present-day understanding, corresponds to a portion of newly formed oceanic lithosphere as a result of mantle upwelling above the young subduction zone.*
b) Joint deformation, at the base of the ophiolite, of the banded peridotites and of the top of the downgoing crust/lithosphere, i.e. the metamorphic sole (see Fig. 9g).
c) The formation of the metamorphic sole marks the mechanical resistance to the initiation of the subduction process, compared here to stripping the nail.
d) The successive accretion of the tectonic slivers making up the metamorphic sole, progressively colder and with a larger sedimentary content (schematically from 1 to 3; see Fig. 9g), reveals a progressively shallower stripping or offscraping of the slab along with a cooling subduction regime.
e) This evolution of accretion accompanies the gradual lubrication and unzipping of the subduction plate boundary, enabling the downward progress of the slab. See text for details.
f) Slabitization, from subduction nucleation to stable subduction. This tectonic scenario relies on observations from sole-peridotite pairs across the world, and uses observations from subduction initiation across the Izu-Bonin/Marianas forearc (e.g., Stern et al., 2012 and references in text). It links early slab dynamics with the onset and progressive downward migration of viscous coupling as the subduction zone cools, and with the onset of mantle upwelling.

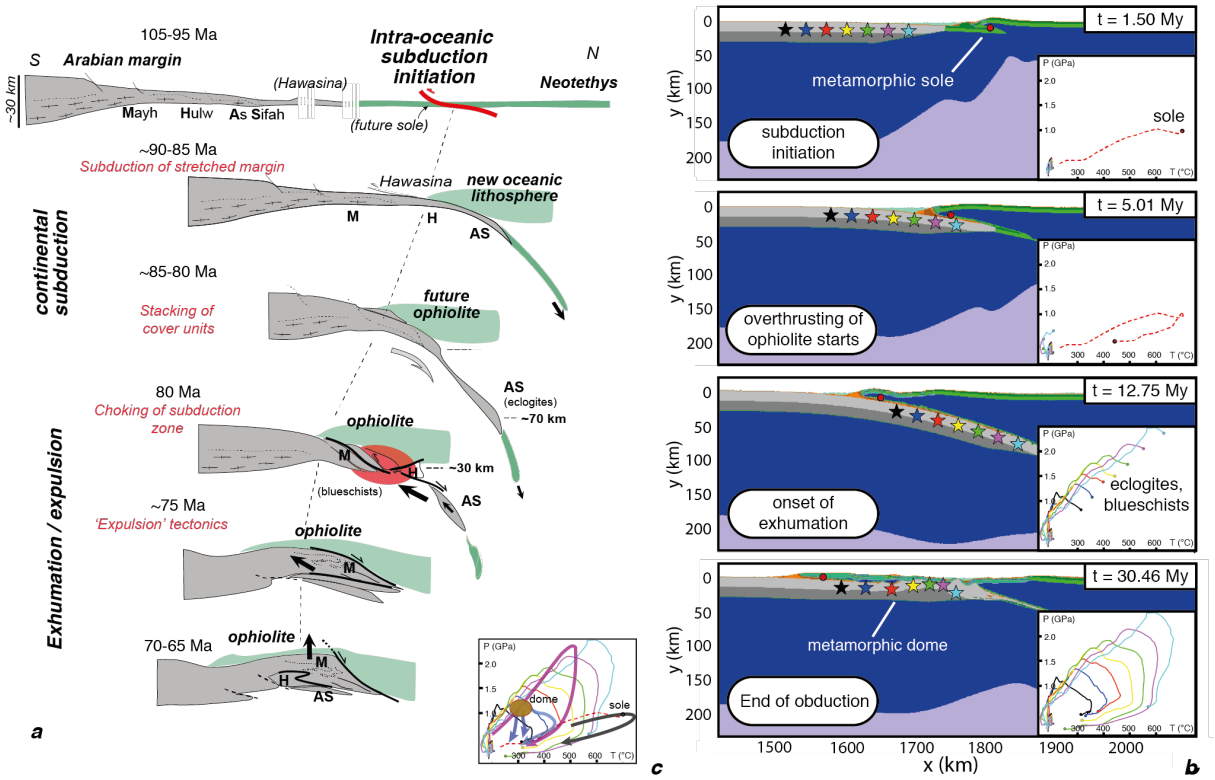

Fig. 12. *a) Geodynamic reconstruction based on the P-T-t paths of the metamorphic sole and of the continental blueschists and eclogites found in the Saih Hatat metamorphic dome, as well as on the sedimentary, stratigraphic and kinematic record (after Agard et al., 2010).*
b) Fully coupled thermomechanical models of obduction (Duretz et al., 2016). Stars outline the evolution and P-T-t paths of some model markers at depth. c) The comparison between predicted P-T-t paths and those estimated from mineral transformations (see Fig. 9j) allows placing constraints on convergence rates, lithosphere ages or rheologies.

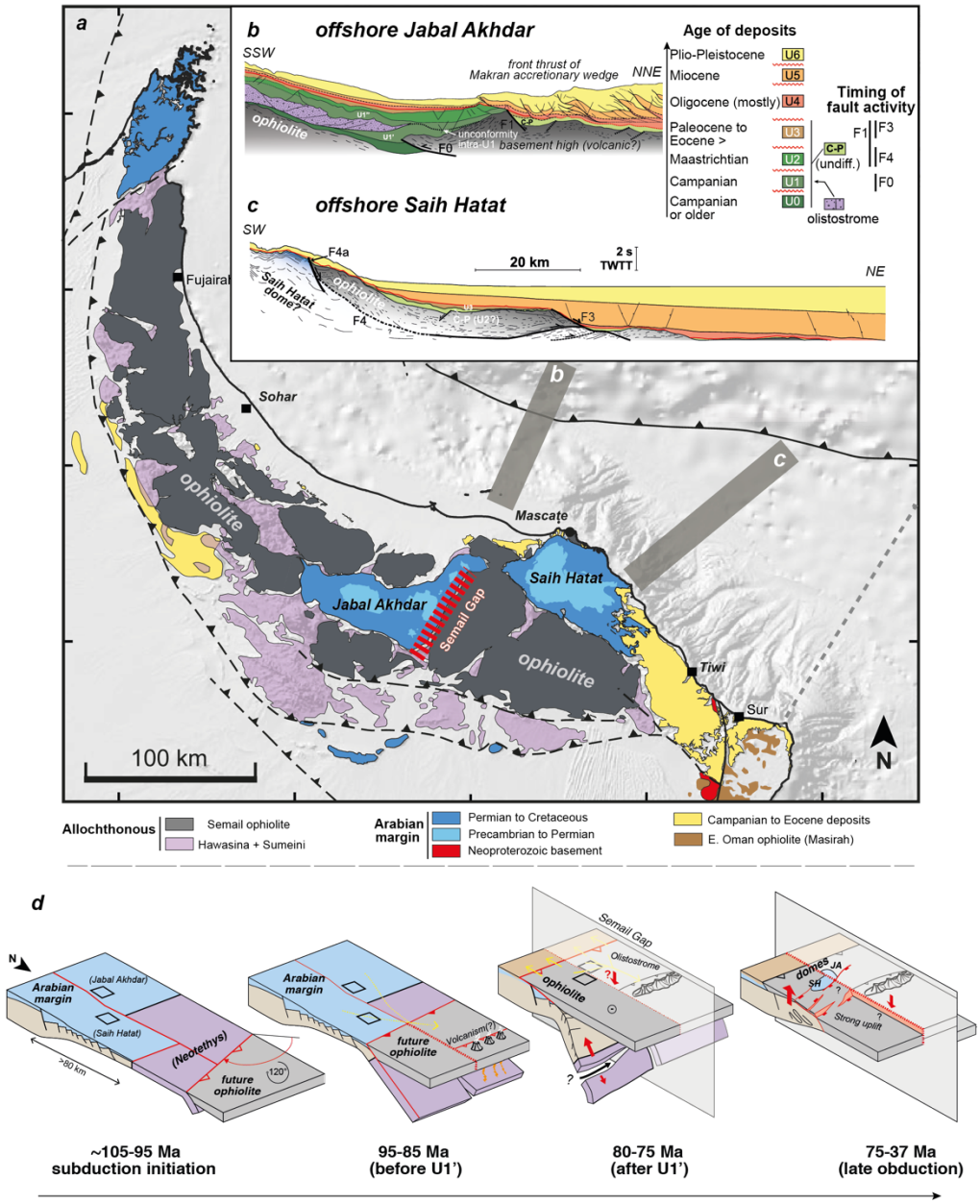

Fig 13. *a) Simplified geological map of northeastern Oman and United Arab Emirates*
b-c) Selection of interpreted seismic profiles across the offshore northern Oman margin (Ninkabou et al., 2021) highlighting the sharp contrasts in sedimentary and tectonic evolution across the Semail Gap, a major crustal-scale divide inherited from the Panafrican orogeny.
d) Obduction and continental subduction of the Oman margin through time. The metamorphic, tectonic and sedimentary records reveal important lateral contrasts across the Semail Gap.

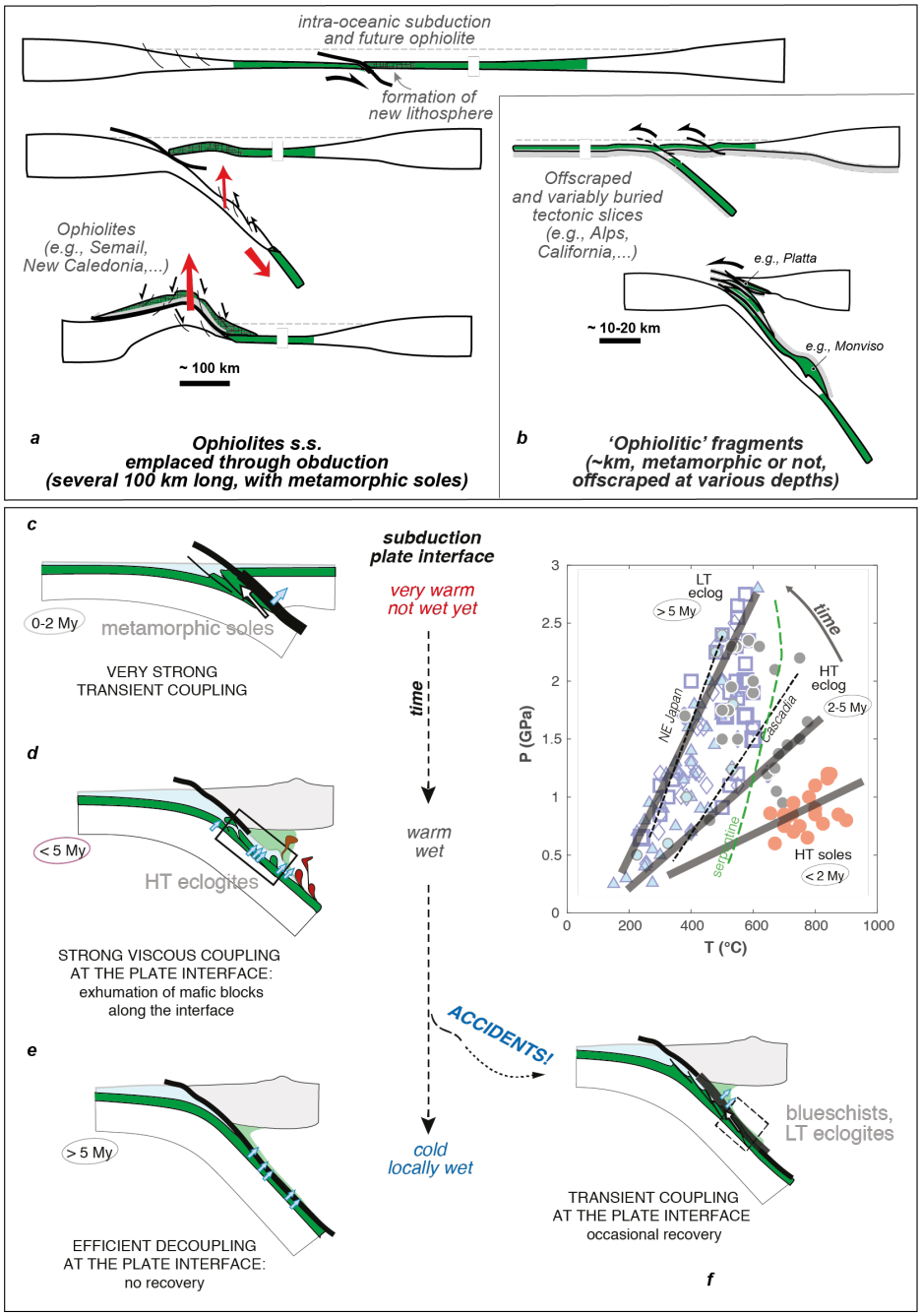

Fig. 14. *a-b) Distinguishing real ophiolites from fragments/slivers/slices of oceanic lithosphere (sometimes referred to as 'ophiolitic') is a matter of scale... and of quite distinct geodynamic context!*
c-f) Long-term trend in mechanical coupling and rock recovery associated with subduction cooling illustrating the fundamental link between metamorphic soles and blueschists and eclogites. The progressive change in mechanical coupling, from strong to weak, is governed by an increase in the effective viscosity contrasts across the subduction interface. The combined evolution of temperature and fluid migration, and fluid storage in the upper plate notably as serpentinite, plays a key role. When young and still relatively dry (c), the plate interface experiences strong viscous coupling, resulting in the offscraping of metamorphic soles. During subsequent subduction and cooling (d) high-temperature eclogite-facies rocks are recovered, mostly in serpentinite mélanges. The steady-state, locally fluid-rich, colder, older and weaker interface leads to a decoupled plate interface (e), similar to most subduction zones today, except during occasional 'accidents' (f) as for the Alps (§ 3; see also Agard et al. 2018 for details).

Ophiolite	Formation age (Ma)	onset of obduction (Ma)	Type	Approx. size (km)	References*
Bay of Islands, **Newfoundland**	485	460	MOR (back-arc?)	>>100x30	*Suhr and Cawood, 1993; Dewey and Casey, 2013*
Coast Range, **USA**	170-165	165-160	SSZ	400x40	*McLaughlin et al., 1988; Choi et al., 2008*
Josephine, **USA**	165-160	155-150	SSZ	100x15	*Harper et al., 1994; Harper, 2003*
Lizard, **England**	>375	370-365	MOR	20x15	*Jones, 1997; Strachan et al., 2014*
Lycian nappes, **Turkey**	100-95	95-90	SSZ	200x50	*Celik et al., 2011; Plunder et al., 2016*
Mirdita, **Albania**	175-165	165-160	SSZ	200x25	*Nicolas et al., 1999; Dilek et al., 2007*
Nappe des péridotites, **New Caledonia**	100, 80?	55	SSZ (forearc) + MOR	300x50	*Ulrich et al., 2010; Cluzel et al., 2012*
PUB, **Papoua-New Guinea**	70-65	60-55	MOR	400x40	*Davies and Jacques, 1984; Lus et al., 2004*
Semail, **Oman-UAE**	96-95	95-90	SSZ	500x100	*Nicolas et al., 2000; Rioux et al., 2012*
Sevan, **Armenia**	165	95-90	MOR	100x30	*Galoyan et al., 2009; Hassig et al., 2016*
Sistan, **Iran**	110-100	70	MOR	300x25	*Zarrinkoub et al., 2012; Jentzer, 2020*
Tanimbar, **Timor**	10-5	5-2	SSZ (forearc)	150x20	*Linthout et al., 1997; Kaneko et al., 2007*
Troodos, **Cyprus**	100-95	95-90	SSZ	50x15	*Moores and Vine, 1971; Pearce and Robinson, 2010*

**for a larger compilation see also Furnes et al., 2014*

Table 1. *Selected list of the most characteristic and well-studied ophiolites in the world.*